PEOPLE'S DEMOCRATIC REPUBLIC OF ALGERIA
Ministry of Higher Education and Scientific Research

University of Amar Telidji - Laghouat FACULTY OF TECHNOLOGY

MECHANICAL ENGINEERING DEPARTMENT

MEMORY

Presented to Obtain the MASTER Diploma in Mechanical Engineering

Specialty: Energetic Mechanics

GUERGAB Amer & ZONBOUT Abou Baker

THEME

Study of the nature of the particle distribution coefficient function in the boundary layer of the sand cloud

Jury :

President :	BELHADJ. M	University of Laghouat
Superviser :	HADJ AISSA Aissa	University of Laghouat
Examiner :	HAMDI. N	University of Laghouat

Academic year: 2023/2024

Abstract:

In this work, we carried out a numerical study of the nature of the particle distribution coefficient function in the boundary layer of the sand cloud. The numerical resolution was done by COMSOL Multiphysics is a finite element analyzer and simulation software package for various physics and engineering applications, especially coupled phenomena and Multiphysics. The results confirm that particle concentration decreases exponentially with altitude. The variation of the diffusion coefficient of sand particles (Dmd) with height direction can be traced as a Gaussian distribution, We found that the diffusion values converged between the two values corresponding to Sct = 0.6 and Sct = 0.9. when the velocity is constant at 10 m/s. While there is a convergence in the values of Sct = 0.3 and Sct = 0.6 when the velocity is constant at 12 m/s. We conclude that the Schmidt number directly affects diffusion. Based on the results obtained from the different diffusion values diffusion we conclude that Schmidt number Sct=0.6 is the most approximate value for the studied phenomenon. We found that when the velocity changes (u= 10 m/s, u= 12 m/s), and we change the Schmidt number, the Schmidt number does not directly affect the concentration. According to the ratio of Schmidt number, it describes the relationship between the rates of turbulent momentum transport and turbulent mass transport, which can explain the effect of wind kinetic energy on the sand turbulent diffusion profiles. The mixture approach application is in good agreement with previous wind tunnel works. This approach can be applied to study the turbulence properties in the Aeolian sand transport.

Keywords: the sand cloud, Aeolian sand transport, Coefficient of tubulation, diffusion, Schmidt number, simulation.

Résumé :

Dans ce travail, nous avons réalisé une étude numérique de la nature de la fonction du coefficient de distribution des particules dans la couche limite du nuage de sable. La résolution numérique a été réalisée par COMSOL Multiphysics, un progiciel d'analyse et de simulation par éléments finis pour diverses applications de physique et d'ingénierie, en particulier les phénomènes couplés et la multiphysique. Les résultats confirment que la concentration de particules diminue de façon exponentielle avec l'altitude. La variation du coefficient de diffusion des particules de sable (Dmd) avec la direction de la hauteur peut être tracée comme une distribution gaussienne. Nous avons constaté que les valeurs de diffusion convergeaient entre les deux valeurs correspondant à Sct = 0,6 et Sct = 0,9. lorsque la vitesse est constante à 10 m/s. Alors qu'il y a une convergence dans les valeurs de Sct = 0,3 et Sct = 0,6 lorsque la vitesse est constante à 12 m/s. Nous concluons que le nombre de Schmidt affecte directement la diffusion. Sur la base des résultats obtenus à partir des différentes valeurs de diffusion, nous concluons que le nombre de Schmidt Sct=0,6 est la valeur la plus approximative pour le phénomène étudié. Nous avons constaté que lorsque la vitesse change (u= 10 m/s, u= 12 m/s) et que nous modifions le nombre de Schmidt, le nombre de Schmidt n'affecte pas directement la concentration. Selon le rapport du nombre de Schmidt, il décrit la relation entre les taux de transport de quantité de mouvement turbulent et de transport de masse turbulent, ce qui peut expliquer l'effet de l'énergie cinétique du vent sur les profils de diffusion turbulente du sable. L'application de l'approche par mélange est en bon accord avec les travaux antérieurs en soufflerie. Cette approche peut être appliquée pour étudier les propriétés de turbulence dans le transport de sable éolien.

Mots clés : nuage de sable, transport de sable éolien, coefficient de tubulation,
diffusion, nombre de Schmidt, simulation**.**

ملخص :

قمنا في هذا العمل بإجراء دراسة عددية لطبيعة دالة معامل توزيع الجسيمات في الطبقة الحدودية للسحابة الرملية. تم إجراء الدقة العددية بواسطة COMSOL Multiphysics وهو عبارة عن محلل العناصر المحدودة وحزمة برامج محاكاة لمختلف تطبيقات الفيزياء والهندسة، وخاصة الظواهر المقترنة والفيزياء المتعددة. تؤكد النتائج أن تركيز الجسيمات يتناقص بشكل كبير مع الارتفاع. يمكن تتبع تباين معامل الانتشار لجزيئات الرمل (Dmd) مع اتجاه الارتفاع كتوزيع غاوسي، حيث وجدنا أن قيم الانتشار متقاربة بين القيمتين الموافقتين لـ Sct = 0.6 و Sct = 0.9. عندما تكون السرعة ثابتة عند 10 م/ث. في حين أن هناك تقارب في قيم Sct = 0.3 وSct = 0.6 عندما تكون السرعة ثابتة عند 12 م/ث. نستنتج أن رقم شميدت يؤثر بشكل مباشر على الانتشار. وبناء على النتائج التي تم الحصول عليها من قيم الانتشار المختلفة نستنتج أن رقم شميدت Sct=0.6 هو القيمة الأكثر تقريبية للظاهرة المدروسة. لقد وجدنا أنه عندما تتغير السرعة (ش= 10 م/ث، ش= 12 م/ث)، ونغير رقم شميدت، فإن رقم شميدت لا يؤثر بشكل مباشر على التركيز. وفقا لنسبة رقم شميدت، فهي تصف العلاقة بين معدلات نقل الزخم المضطرب والنقل الجماعي المضطرب، والتي يمكن أن تفسر تأثير الطاقة الحركية للرياح على ملامح انتشار الرمال المضطربة. إن تطبيق نهج الخليط يتوافق بشكل جيد مع أعمال نفق الرياح السابقة. يمكن تطبيق هذا النهج لدراسة خصائص الاضطراب في نقل الرمال الإيولية.

الكلمات المفتاحية: السحابة الرملية، انتقال الرمال الإيولية، معامل الأنابيب، الانتشار، رقم شميدت، المحاكاة.

Acknowledgments

Gratitude towards people is a form of gratitude to God. We must express sincere thanks for noble efforts, even if they are duties, I would like to express my sincere gratitude to my supervisor, HADJ AISSA Aissa, for his continuous support, patience, and guidance throughout my research. His insightful feedback pushed me to sharpen my thinking and brought my work to a higher level. I am also grateful to the members of my dissertation the president. BELHADJ .M and the examiner. HAMDI. N committee for their valuable comments and suggestions, which greatly improved my work. We pray that the Almighty rewards you for your tremendous efforts in ensuring the success of the final examinations. Your tireless work with the students and successful conclusion of the academic year deserves the highest honor and appreciation. Despite our words, we cannot fully repay you, so we offer our prayers for your continued success and prosperity. You have our utmost respect and gratitude.

Dedications

We dedicate this modest work:

To our parents.

To our brothers and sisters.

To all family and friends.

Table of Contents

Table of Figure

Nomenclature

C_d : mass fraction of the dispersed phase, (kg/kg)

D_{md} : turbulent dispersion coefficient, (m^2/s)

dp: sand particles diameter

g: gravitational acceleration, (m/s^2)

k: kinetic energy of turbulence, (m^2/s^2)

n: conservation of the number density($1/m^3$)

P: pressure of mixture flow (Pa)

U: velocity of mixture flow (m/s)

u_c : velocity vector of the continuous phase (m/s)

u_d : velocity vector of the dispersed phase (m/s)

u_{slip} : relative velocity between the two phases (m/s)

Greek Symbols

ε : dissipation energy of turbulence (m^2/s^2)

μ_T : mixture turbulent viscosity (Pa. s)

ρ : density of mixture flow (kg/m^3)

ρc : density of the continuous phase (kg/m^3)

ρd; density of the dispersed phase (kg/m^3)

σ_T: turbulent particle Schmidt number

τ_{Gm}: sum of the turbulent and viscous stresses ($kg/(m \cdot s^2)$)

$\emptyset_{\mathbf{c}}$: volume fractions of the continuous phase (m^3/m^3)

$\emptyset_{\mathbf{d}}$: volume fractions of the dispersed phase (m^3/m^3)

General Introduction

Sand clouds, also known as aeolian dust storms, are common natural phenomena occurring in arid and semi-arid regions worldwide. These events result from the suspension and transport of sand and dust particles by wind, creating expansive clouds that can travel significant distances and affect various environmental and human systems. Understanding the behavior of sand clouds is essential for predicting their impact on air quality, climate, agriculture, and public health.

One critical aspect of sand cloud dynamics is the behavior of particles within the boundary layer, the region of fluid flow adjacent to the Earth's surface where frictional effects significantly influence airflow. Within this boundary layer, the distribution of sand particles plays a crucial role in determining the magnitude and extent of sand cloud phenomena. The particle distribution coefficient function provides valuable insights into how sand particles of different sizes and densities are distributed within this layer.

The particle distribution coefficient function describes the relationship between the concentration of particles of a specific size and their position within the boundary layer. This function is influenced by various factors, including the size distribution of sand particles, wind speed and direction, turbulence, atmospheric stability, and surface roughness. Understanding the nature of this function is vital for accurately modeling and predicting the behavior of sand clouds.

This study aims to investigate the nature of the particle distribution coefficient function within the boundary layer of sand clouds. By numerical simulations. The first chapter deals with definitions and a bibliographic review , In the second chapter, we discuss the physical problem and mathematical formulation. The third section addresses the numerical method and simulation and The final chapter presents the results and discussion.

Our research aims to contribute to a deeper understanding of sand cloud dynamics and provide valuable insights for improving predictive models and mitigation strategies for sandstorm events.

Chapter I : Definitions and Bibliographic Review

I.1. Aeolian Sand transport phenomena:

I.1.1. Background

Uncontrolled, powerful, or turbulent winds combined with exposed, loose, dry surfaces result in sand and dust storms SDS. These ailments are widespread in semiarid and arid areas. Sandstorms happen relatively close to the surface of the Earth, but smaller dust particles can be propelled miles into the air by powerful winds, where they can travel great distances and even cover continents. Governments and the worldwide community are become more concerned about SDS due to its negative effects on agriculture, infrastructure, transportation, and human health. Policy-makers need to know the answers to three key questions: (i) have dust storms gotten worse recently? (ii) how much of SDS is caused by human activity? (iii) and what can be done to stop them and protect us from their effects? Although exact figures are very difficult to determine, approximately 75% of current worldwide dust emissions are due to nonanthropogenic, natural causes. These topographical depressions in arid areas are primarily dry, old lake bottoms with scant flora. About 25% of the world's dust emissions are attributable to anthropogenic sources, which are primarily (85%) hydrological sources (ephemeral waters). For SDS mitigation methods, the predominance of natural sources and a rising threat of greater anthropogenic inputs have significant ramifications. [1]

Unsustainable land use and degraded soil, particularly in semi-arid regions, greatly increase the likelihood of increasing wind erosion, which can negatively impact agricultural yield even in the absence of SDS production. By serving as a mechanical barrier, limiting wind flow, and decreasing surface shear stress at the soil surface and by physically defending the soil surface, vegetation acts as a protective mechanism. It also increases soil stability by recycling organic matter. [1]

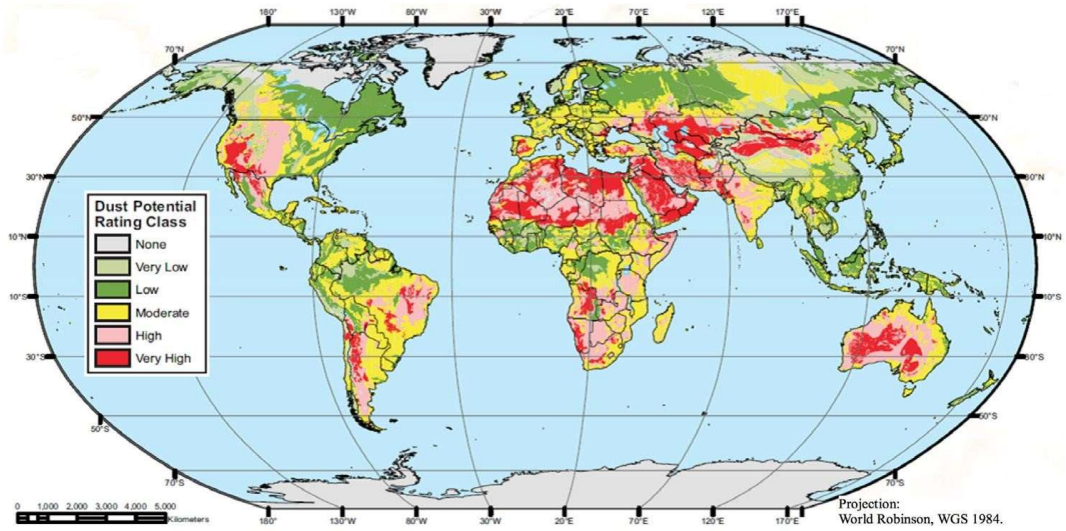

Figure I- 1 : Global Dust Potential Map. [Source: DTF (2013)].

I.1.2. Definition:

Aeolian processes are those processes of erosion, transport, and deposition of sediments that are caused by wind at or near the surface of the earth. Sediment deposits produced by the action of wind and the sedimentary structures characteristic of these deposits are also described as aeolian.

Aeolian processes are most important in areas where there is little or no vegetation. However, aeolian deposits are not restricted to arid climates. They are also seen along shorelines; along stream courses in semiarid climates; in areas of ample sand weathered from weakly cemented sandstone outcrops; and in areas of glacial outwash.

Loess, which is silt deposited by wind, is common in humid to subhumid climates The lee (downwind) side of river valleys in semiarid regions are often blanketed with sand and sand dunes. Examples in the Deserts of Algeria [19]

Figure I- 2 : Sand storm on the borders of Laghouat and Ghardaia, Algeria

I.1.3. Physical processes and modes of wind-blown sand transport

These processes (creep, reptation and saltation) produce an exponential increase in the particle concentration, which leads to increasing drag on the wind, thereby retarding the wind speed in the saltation layer. It is this slowing of the wind that acts as negative feedback by reducing particle speeds, and thus the splashing of new particles into saltation, which ultimately limits the number of saltating particles and thereby partially determines the characteristics of steady state saltation. [20]

Very small particles are predominantly ejected from the soil by the impacts of saltating particles. Following ejection, dust particles are susceptible to turbulent fluctuations and thus usually enter short-term or long term suspension. Very small particles (fine fraction) ranging from **63** to **100 μm** are transported in suspension by turbulent

eddies. Sand particles between **100** and **300 μm** are mostly transported by making saltation (small hops). The largest particles (coarse fraction) ranging from **300** to **2000 μm** are transported by sliding and rolling as surface creep. The transport of particles by rolling, sliding and small hops (saltation's) can be defined as bed load transport of particles in more or less continuous contacts with the bed. Bed load transport of particles in a thin transport layer is the dominant mode of transport for sand particles (100 to 300 μm) in air. Observations in wind tunnels and in nature show that most of the transport occurs in a thin layer (< 0.05 m) above the sand surface (Ho, 2012.). In this thin transport layer, the particle velocity (averaged over the layer thickness) is almost insensitive to the external wind velocity above the transport layer and approximately equal to the 3 to 4 times the threshold bed shear velocity (up≅ 3 to 4 u*,cr). Particle concentration is so high that the wind velocity is strongly reduced to a value of the order of 0.8 to 1.2 m/s (Kok et al., 2012). An increase of the wind velocity results in an increase of the particle concentration which in turn leads to a decrease of the wind flow speed close to the bed such that the new equilibrium particle velocity remains almost unchanged . [20]

Above the saltation layer, the suspended particle concentrations are much smaller, and the air flow is almost unaffected by the presence of the particle. As a result, the particle velocity above the saltation layer increases with increasing wind velocity

A flat sand bed exposed to a wind strong enough to set grains into motion is unstable. That is, saltation over an initially flat sand bed results in the generation of two types of bedforms with distinct length scales: ripples with length scales of up to 1000d50 and dunes, which are typically 5 to 10 meters high but can reach lengths of 100 to 300 m. Dunes occur frequently as isolated objects moving on a firm ground (such as barchan dunes in a corridor) but also as multiple dunes evolving on a dense sand bed. Ripples appear most commonly on the surface of dunes as chains of small undulations that orient transversely to the wind trend. Many insights have been gained during the last few decades from computer modelling. [20]

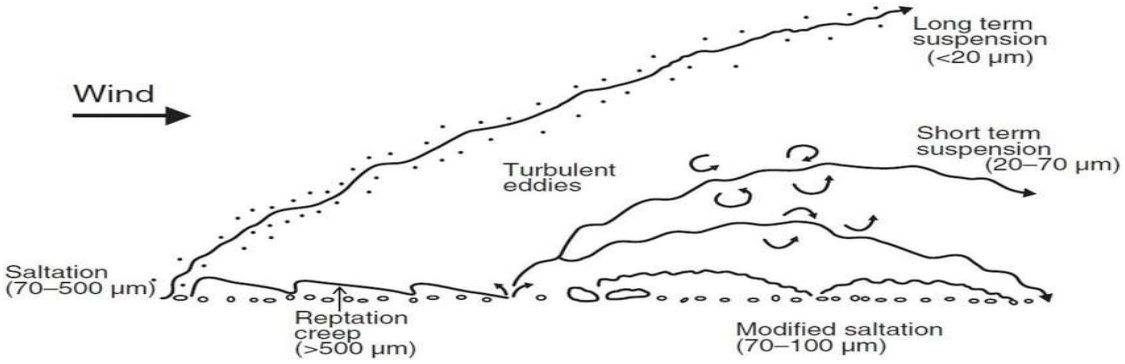

Figure I- 3 : Schematic of the different modes of aeolian transport.

I.1.4. Condition and trends:

SDS are identified and monitored by combining computational modelling, ground surveillance data, and satellite photography. The Northern Hemisphere is home to the biggest concentrations of high levels of dust, both naturally occurring and caused by human activity. This is particularly true of a huge dust belt that stretches from China to the west coast of North Africa to the Middle East, Central Asia, and South Asia. Although these sources have significant local effects, the southern hemisphere does not exhibit significant dust activity, with modest concentrations in central Australia, southern Africa, the Atacama in South America, and the Great Basin in North America. The southern Sahel has more anthropogenic dust sources, which are assumed to be mostly related to agriculture and grazing operations, compared to the Sahara, which is the most significant producer of dust globally and is essentially natural. Additionally, human sources predominate in the Atlas Mountains and along the Mediterranean coast. [1]

Mesopotamia is a significant source region in the Middle East, which displays a complex mixture of anthropogenic and natural sources. The Etosha and Makgadikgadi Basins in Southern Africa are two of the three major dust generators in the Southern Hemisphere. Except for a few transient lakes, the majority of dust activity in North America occurs in the vast plains that run from southern Texas to Montana. The Atacama Desert in Chile and Peru is South America's greatest natural source, whereas Argentine Patagonia is the region with the most human-made sources. The Indian subcontinent's northern region is a significant producer of dust, largely because of ephemeral bodies of water generated by land usage that range in size from huge rivers to tiny lakes. On the border between Iran, Pakistan, and Afghanistan, dust storms are prevalent. The greatest natural springs in East Asia are located in basins in China, including the Taklamakan Desert. [1]

According to simulations, a combination of land use and climate change over the past century has resulted in an increase in yearly worldwide dust emissions of 25% to 50%. Over the past few decades, SDS has become more common and severe in certain places while declining in others. Over the previous three decades, there don't seem to have been any significant changes in dust activity over North Africa, the Middle East, or South America, but there have been significant changes over the US Plateau, Central Asia, and Australia. [1]

There is evidence to suggest that better land management helps certain places reduce SDS. According to climate change forecasts, the majority of Mediterranean Europe and Africa, the northern Sahara, central and western Asia, the US southwest, and southern Australia are among the locations that are already dusty and are predicted to grow drier. Since 1950, precipitation has increased in northern hemisphere mid-latitude land regions, which may help slow the midlatitude belt's desertification. East Africa and East Asia are dusty regions that are predicted to grow wetter, but Sahel-Sudan, the Gangetic Basin, and the Lake Eyre region cannot be projected due to substantial model uncertainty.[1]

I.2. Transport of Sand by Wind (Aeolian Transport):

I.2.1. Definition

There are three forces that determine if, and how, an individual grain of sediment will be transported by wind (fig I-4). Gravity acts to keep the grain at the ground surface (FG), there is a drag component that moves the grain along the ground surface (FD) with the wind direction and a lift force (or shear stress: FL) produced by pressure differences created by the movement of wind over the surface of a stationary grain. This lift force is the result of a relatively high velocity flow across the top of the particle, and lower velocities across the middle and lower parts of the sand grain. A stationary grain will begin to first vibrate, and then move when the shear stress at the grain surface exceeds a specific critical value (i.e., the vertical lift exceeds gravitational force, FL>FG) (fig I-4). [18]

I.2.3. Particle Flow Equation

This equation describes the movement of individual particles in granular flow and relies on the balance between the forces acting on the particle and the driving forces. [18]

$$Fd = Fg + Fl + Fv + Fin \quad \text{(I-1)}$$

Where:

Fd: is the drag force exerted on the particle due to the airflow.

Fg: is the gravitational force acting on the particle due to gravity.

Fl: is the lift force generated by the airflow around the particle.

Fv: is the virtual lift force generated by the airflow around the particle, which is considered hypothetical.

Fin: is the inertial force resulting from acceleration and changes in velocity of the particle. [18]

These forces are influenced by factors such as the shape and size of the particle, its density, the velocity of the airflow, and other environmental conditions

1.Bagnold's Equation :This equation describes the wind velocity necessary to move sand grains and depends on factors such as grain weight, wind speed, and grain size.

2.Lozneanu's Equation: This equation describes the wind force required to move a sand grain, and it depends on factors such as the shape and size of the grain and wind speed. These equations are some of the well-known examples used in studying sand movement under the influence of wind. [18]

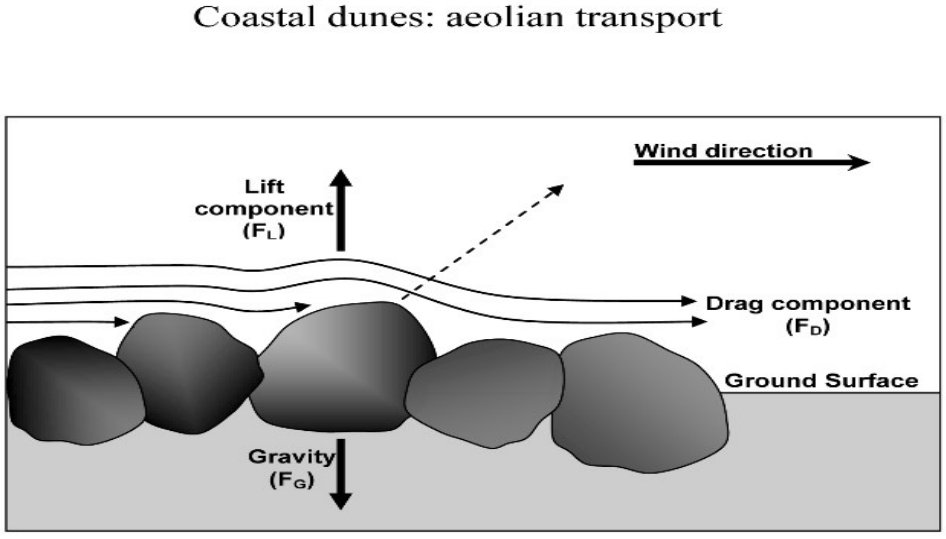

Figure I- 4 : Forces operating in the process of sand sized sediment entrainment

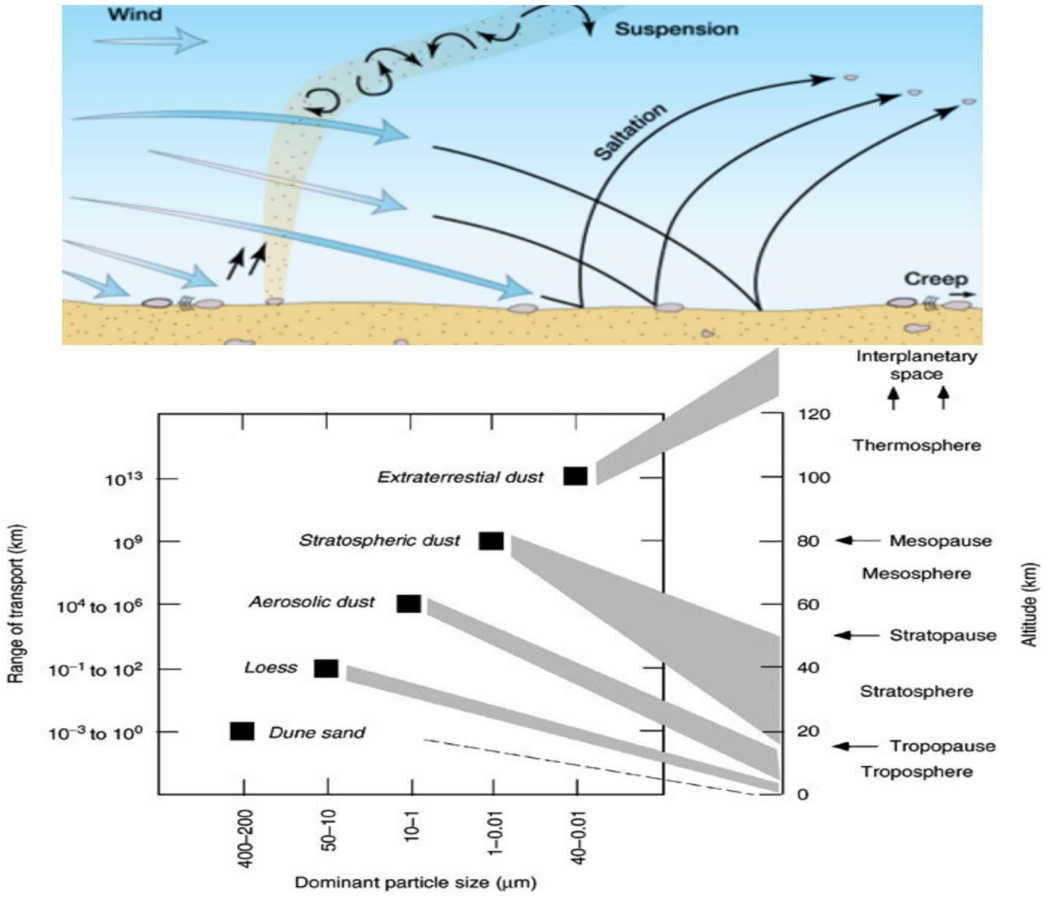

Figure I- 5 : Aeolian environments

I.2.4. Overall picture

The Northern Hemisphere (Figure I-6) is home to the biggest concentrations of high aerosol levels, both from natural and anthropogenic causes. This concentration is mostly found in a broad dust belt that stretches from China to the west coast of North Africa, to the Middle East, Central and South Asia, and the Middle East. There is very little significant dust activity outside of this area. Although SDS occurrences are significant in terms of their local consequences, the southern hemisphere in particular does not demonstrate significant dust activity. Lower amounts can be found in the North American Great Basin, the Atacama Desert in South America, central Australia, southern Africa's Botswana, and Namibia. [1]

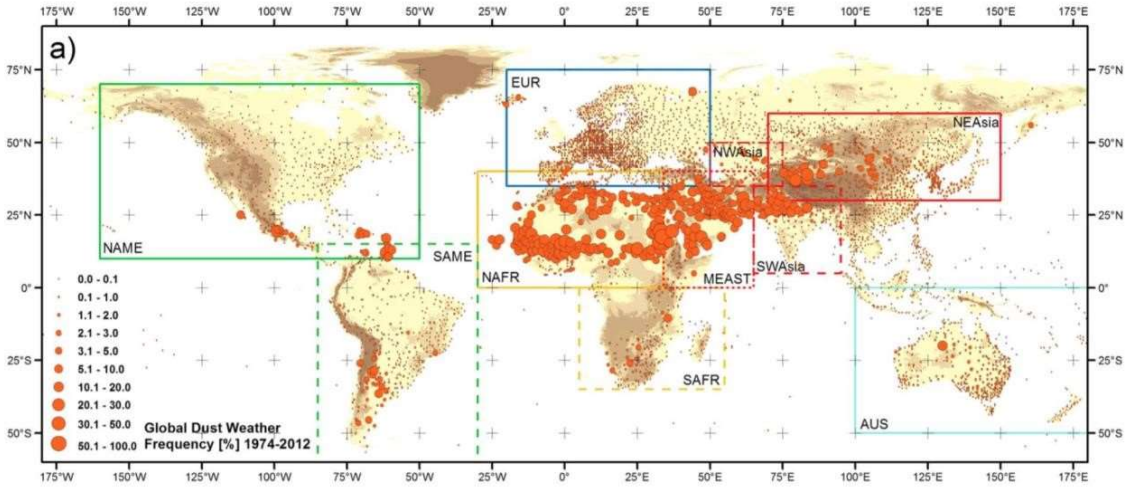

Figure I- 6 : The synoptic current weather records for the period of January 1974 to December 2012 were used to determine the global pattern of dust frequency. Shao et al. (2013) as the source

Most desert dust is emitted from natural sources with little influence from humans and the relative contributions from global dust sources that are significantly influenced by human activities have a large uncertainty, ranging from less than 10% to 50% of global emissions, but are most likely around 25%. Deposition rates associated with some of the main dust lanes indicate high rates along the Niger River in Mali. According to MODiS Deep Blue data, ephemeral water bodies and other hydrological dust sources account for 31% of worldwide emissions, 15% of which are natural and 85% of which are human partly vegetated surfaces account for around 20% of emissions, primarily agricultural land and scrubland in the desert. [1]

In topographical depressions in dry areas, thick alluvial deposits created by periodic floods during the Quaternary and into the Holocene represent the majority of the principal producers of dust [1]

The alluvium layer is deep enough in some of these depressions to support dust emission without further filling, but in others, flooding frequently creates fresh sediment deposits, which subsequently serve as potential sources.

ephemeral lakes and riverbeds are frequently active producers of dust. [1]

I.2.5. Research in Wind Tunnels

Studies conducted in wind tunnels have the significant benefit of enabling tests to be carried out in a controlled laboratory environment. Compared to usual field scenarios, it is simpler to regulate the number of variables functioning at once, and conditions can be maintained long enough for experiments to be completed and repeated. The primary negatives are related to scale issues, however, if necessary, safeguards are followed, this need not diminish the usefulness of modelling work. [1]

The majority of laboratory wind tunnel studies of aeolian processes have focused on grain-bed interactions, the nature of particle trajectories, and the threshold for particle entrainment .

However, laboratory wind tunnels have also been used to study airflow over model dunes, the impact of obstructions on sand deposition, and the production of micro-dunes under simulated Yeniseian atmospheric conditions

There have been two different kinds of lab wind tunnels employed. The first is an open-circuit tunnel, which typically consists of three components: a diffuser, a test section, and an entry cone. A fan situated at the diffuser's end draws air in via the bell-shaped opening. As a result, there are less airflow disruptions inside the tunnel, which may be a major issue in tunnels using blower fans .[1]

The open-circuit tunnel is often kept inside a building since it is susceptible to outside winds.

Figure I- 7 : Wind tunnel experiment setup [University of Lethbridge, Canada]

The second kind is a closed-circuit tunnel, which is, as its name suggests, sealed and has an air flow that circulates continually, employed this sort of tunnel mostly for aeolian abrasion studies and simulations of sediment transport at high pressures.

A variety of natural soils and sediments have been studied in open-floored wind tunnels in order to establish threshold velocities and the correlation between shear velocity and particle flux

It is crucial to make sure that the wind tunnel's circumstances are an accurate representation of those found in the real world. Therefore, care should be made to guarantee that:

-Any model dune or barrier to the flow has the exact same geometry as the actual.

-The vertical wind velocity profile and degree of turbulence are typical of the flow conditions that occur in nature.

-The test segment is long enough to allow for homogeneous sand transport rates, and all the factors that impact sediment transport are scaled appropriately to preserve dynamic similitude. [1]

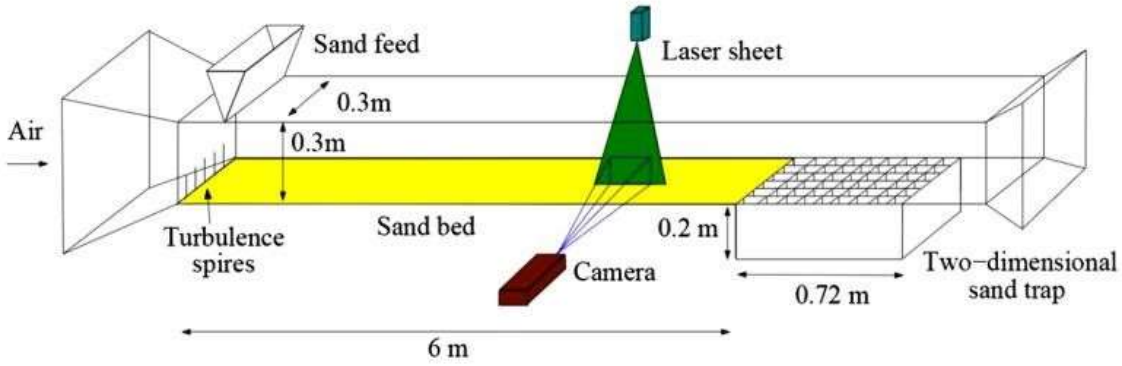

Figure I- 8 : Wind tunnel used by Ho et al. For characterizing the saltation transport using Particle Image Velocimetry and sand trap system

If the tunnel floor is roughened for a significant distance upwind of the test section, a thick boundary layer forms in the wind tunnel naturally. For this, an extremely long wind tunnel with a significant fetch in front of the test portion is necessary. With enough depth, such a naturally formed boundary layer exhibits outstanding agreement with atmospheric data .

However, a substantial boundary layer may be produced in short wind tunnels by positioning a velocity profile generator upwind of the test area, this may take the form of a grid with smaller openings close to the tunnel's bottom and bigger openings farther up the wall. As an alternative, a bent wire-mesh screen placed with its vertical edges close to the roof and its horizontal edges close to the ground will accomplish the same thing.

Using longitudinal vortex generators is another technique for artificially regulating the turbulent boundary layer's expansion. A long fetch of floor roughness and vortex generators are often used to allow a boundary layer to emerge. Sand movement simulation does not need exact replication of natural boundary layer conditions, including flow field temperature stratification.[1]

I.3. Sand concentration

I.3.1. Definition

Sand concentration is the amount of sand in the liquid or gas. Sand concentration can affect the properties of the liquid or gas, such as viscosity, density, and pressure. Sand concentration is important in some applications, such as hydraulic fracturing, sand management, and erosion.

There are some methods to calculate sand concentration, depending on the type of liquid or gas and the size of sand particles. Some examples are:

In hydraulic fracturing, equations are used to calculate sand rate, liquid rate, nitrogen rate, and horsepower. For example, sand rate can be calculated by the following formula:

$$\text{Sand rate} = \frac{sand\ concentration \times liquid\ concentration}{100} \qquad (I.2)$$

Where sand concentration is the ratio of sand weight to liquid weight in percentage, and liquid rate is the volume of liquid pumped per minute in barrels.

In sand management, sensors and meters are used to measure sand concentration, particle size, and flow velocity For example, sand concentration can be calculated by the following formula:

$$\text{Sand concentration} = \frac{Mass\ \ flow\ of\ sand}{Mass\ flow\ rate\ of\ liquid}.. \qquad (I.3)$$

Where mass flow rate is the mass of liquid or sand passing per unit time.

In erosion, impact factors such as velocity, angle, density, and hardness are used to estimate erosion rate due to sand. For example, erosion rate can be calculated by the following formula:

$$\text{Erosion rate} = K \times \text{Sand concentration} \times \text{Velocity} \qquad (I.4)$$

Where K is the erosion coefficient, and n is the velocity exponent, which depend on the properties of the material and the sand and the angle

I.4. Turbulent Diffusion Coefficient:

I.4.1. Background

Among the parameters that influence particle dispersion are particle size, density, fluid scales, and turbulence structure. It can be indicated that the parameter that characterizes the particle dispersion is the relative mean velocity between the particle and the surrounding fluid, form inversely proportional to it . The diffusion coefficient can be calculated using the definition of the turbulent Schmidt number It can be also defined as the ratio between the kinematic air viscosity ν and the diffusivity Dmd of sand particle[22]

The coefficient describing turbulent diffusion is analogous to molecular diffusivities but lacks a true physical meaning and It depends on flow conditions and is not an inherent property of the fluid it self, in summary, turbulent diffusion plays a vital role in mixing and transport, especially in scenarios where rapid concentration reduction is necessary. Despite challenges, ongoing research aims to enhance our understanding and modeling capabilities in this dynamic field and The turbulent diffusion coefficient is an essential parameter in understanding the transport of mass, heat, or momentum within turbulent fluid systems. [22]

the formula for this coefficient:

The turbulent diffusion coefficient is formulated based on the turbulent Schmidt number (Sc_t):

The Schmidt number characterizes the ratio of molecular diffusivity to turbulent diffusivity.

It is defined as: $Sc_t = \frac{\mu_t}{\rho D_t}$ (I.4)

where:

- μ_t represents the turbulent viscosity.
- ρ is the density of the fluid.
- D_t denotes the turbulent diffusivity.

I.4.2. Significance:

Turbulent diffusion occurs rapidly in turbulent flows, making it crucial for mixing and transport in various scenarios, such as combustion, contaminants, dissolved oxygen, and industrial processes.

While predicting turbulent diffusion remains challenging due to turbulence's complex nature, understanding the coefficient helps us model species transport more effectively.[22]

In fluid dynamics, the Schmidt number (denoted Sc) of a fluid is a dimensionless number defined as the ratio of momentum diffusivity (kinematic viscosity) and mass diffusivity , and it is used to characterize fluid flows in which there are simultaneous momentum and mass diffusion convection processes. It was named after German engineer Ernst Heinrich Wilhelm Schmidt (1892–1975).[22]

The Schmidt number is the ratio of the shear component for diffusivity (viscosity divided by density) to the diffusivity for mass transfer D. It physically relates the relative thickness of the hydrodynamic layer and mass-transfer boundary layer.

It is defined as:

$$\mathrm{Sc} = \frac{\nu}{D} = \frac{\mu}{\rho D} = \frac{\text{viscous diffusion rate}}{\text{molecular (mass) diffusion rate}} \qquad \text{(I.5)}$$

where (in SI units):

D is the mass diffusivity (m2/s).

μ is the dynamic viscosity of the fluid (Pa·s = N·s/m2 = kg/m·s)

ρ is the density of the fluid (kg/m3).

The heat transfer analogy of the Schmidt number is the Prandtl number (Pr). The ratio of thermal diffusivity to mass diffusivity is the Lewis number (Le).

The turbulent Schmidt number is commonly used in turbulence research and is defined as: $\mathrm{Sc_t} = \frac{\nu_t}{K}$ where: - ν_t is the eddy viscosity in units of (m2/s) (I.6)

- K is the eddy diffusivity (m2/s).

The turbulent Schmidt number describes the ratio between the rates of turbulent transport of momentum and the turbulent transport of mass (or any passive scalar). It is related to the turbulent Prandtl number, which is concerned with turbulent heat transfer rather than turbulent mass transfer. It is useful for solving the mass transfer problem of turbulent boundary layer flows. The simplest model for Sct is the Reynolds analogy, which yields a turbulent Schmidt number of 1. From experimental data and CFD simulations, Sct ranges from 0.2 to 6. [22]

the Fickian diffusion assumption based on turbulent diffusivity remains the most widely-applied framework to study the transport of a scalar in a turbulent flow. The assumption of the standard gradient diffusion hypothesis requires the estimation of the turbulent Schmidt number, Sct . This parameter is defined as the ratio of momentum diffusivity to mass diffusivity in a turbulent flow:

$$Sc_{t-i} = \frac{\nu_{t-i}}{D_{t-i}} \quad \text{(I.7)}$$

where νt-i is the eddy kinematic viscosity in the i-th direction. Hence, if the turbulent Schmidt number is known, the turbulent diffusivities can be estimated as:

$$D_{t-i} = \frac{\nu_{t-i}}{Sc_{t-i}} \quad \text{(I.8)}$$

where ν is the molecular kinematic viscosity of the fluid and Dm is the molecular diffusivity of the scalar within the fluid. Therefore, the turbulent Schmidt number Sct is a property of the turbulent flow, whereas the Schmidt number Sc is a property of the fluid and of the substance being diffused within the fluid. The Schmidt number Sc is usually in the order of one and of 102–102 depending on temperature for environmental flows in air and water, respectively on the contrary, since Sct is a characteristic feature of the turbulent flow, no universal value could be established. Hence, by analogy between momentum and mass transport, Sct is often assumed as a first approximation to be equal to unity. However, empirical values different from one have been used in different studies [22]

I.4.3. Values of the turbulent Schmidt number:

A large number of studies has been carried out to identify the best value for the turbulent Schmidt number to be applied in the numerical simulation. A first group of studies was aimed at estimating the most proper value for Sct and at identifying the impact of Sct on the numerical results [21]

Table 1 : Values of the turbulent Schmidt number

Reference	Environmental Flow	Comments
Koeltzsch [3]	Tracer transport in a boundary layer	Exp − Sct = 0.3–1, Sct = Sct (BL height)
Tominaga and Stathopoulos [4]	Review paper	Exp/Num − Sct = 0.2–1.3
Riddle et al. [5]	Pollutant dispersion in the built environment	Exp/Num − Sct = 0.3 and 0.7
Di Sabatino and Buccolieri [6]	Pollutant dispersion in the built environment	Exp/Num − Sct = 0.4 and 0.7
Galeazzo et al. [7]	Jet in crossflow	Exp/Num − Sct = 0.3–0.9
Goldberg et al. [8]	Different type of air flows	Exp/Num − Sct variable
Shi et al. [9]	Density stratified jets	Exp/Num − Sct = Sct (velocity and density gradient)

Koeltzsch [3] reviewed some previous experimental investigations and found that most authors use a constant value for Sct ranging from 0.5 to 0.9.

Tominaga and Stathopoulos [4] reviewed a number of previous studies related to the application of optimum values of Sct for engineering flow fields relevant to atmospheric dispersion, such as jet-in-cross flow, plume dispersion in boundary layer and dispersion around buildings. They found that the optimum values for Sct were widely distributed in the range of 0.2–1.3, and the specific value selected had a significant effect on the prediction results. Since the optimum values of Sct largely depended on the local flow characteristics, they recommended that Sct should be determined by considering the dominant effect in the turbulent mass transport in each case.

Riddle et al. [5] simulated the atmospheric boundary layer flow and plume dispersion from an isolated stack for neutral stability and flat terrain situations. They compared the CFD results about the spread of gas plume with the predictions from the Atmospheric Dispersion Modelling System (ADMS), a well-tested and validated quasi-Gaussian model. They used Sct = 0.7, but found that the CFD predictions were significantly higher (exceeding a factor of two) than expected values. By reducing Sct to 0.3 to increase the plume dispersion, the predicted ground level concentrations were improved, but the horizontal plume spread was still significantly less than expected.

Di Sabatino and Buccolieri [6] compared the CFD simulations with the predictions from a well-validated Gaussian model for the case of dispersion due to the presence of a buildings array. They found the best results for low and high frontal area density when using Sct = 0.7 and 0.4, respectively.

A second group of studies investigated the question if Sct is a constant or it is varying inside the flow domain Koeltzsch [3] carried out wind tunnel experiments in a turbulent boundary layer above a flat plate. The data showed a strong dependence of Sct, which was in the range from 0.3 to 1, on the height within the boundary layer. These experimental data corresponded well with values reported previously when the height used is normalized by the boundary layer thickness, suggesting that Sct should be not considered as a constant in the flow domain

In most of the presented studies, the best-fitting Sct is in the range from 0.1 to 1, but in sediment-laden open channel flows for sand particles, it was found that the best Sct was largely above unity, in the range from 1.4 to 2.1. Thus, it is impossible to identify a unique value for the best-fitting Sct valid for all of the considered cases.

I.4.4. Applications:

• Atmospheric Diffusion and Pollutants:

• Atmospheric dispersion models study how pollutants mix in the environment.

• Both Eulerian and Lagrangian models incorporate vertical and horizontal wind, accounting for turbulence using Fickian diffusion theory.

• Despite assumptions and ideal conditions, accurately calculating turbulent diffusion effects on pollutants remains challenging1.

Chapter II : Physical Problem and Mathematical Formulation

II.1. Mixture model equations

The modelling of differential equations in multiphase flows science is considered big challenges in the simulations of multiphase flows. The Favre-averaged balance equations of the mixture model depending on specific applications were introduced by many authors[M.Ishii,1975][G.Ahmadi,D.Ma,1990][D.Gidaspow,1994][10]. The practical issues related to the mixture model include changing the turbulence model appropriate of single-phase by considering the effect of the particles and determining the shape of the diffusion coefficient that exist in the equation of continuity for the dispersed phase fluid. [S.T.Johansen,N. M.Anderson,1990][11] used the k-ε model to model the turbulence by developing a model based on stationary state close to the model applied in the mixture model. The turbulent stress term was presented as sum of contributions from the two phases and the turbulent viscosity for the two phases was calculated separately, the mixture model was applied to the fine particles within the airflow. it concludes that the particles can exchange momentum with the fluid and change the turbulent structure of the carrier gas. The components of different phase (numerical or real) in mixture model behave like a single fluid flow in terms of total momentum and mass. The properties of fluid such as density, viscosity, etc. are used as in the mixture properties. The species concentration was used to present the equation for each phase, which is formulated to allow the transport of the species through the volume deviating from the usual convective and diffusive terms of the mixture. This motion or drift is introduced into the species equation using an extended flow term, which was responsible about the slip of the phase. The changing of the velocity from mixing to phase reformed the term of normal flow, the force balance on each phase used to calculate the normal flow term. The mixture approach tracks the average phase concentration and calculate the mixture velocity by solving a single momentum equation. The dispersed phase slip velocity is relative to the continuous phase. The slip velocity was calculated based on the balancing between the body and drag forces due to the density difference. The governing equations for continuity and momentum were written for dispersed phase and continuous phase, where the algebraic equations were used to approximated the momentum equations for the sand particles [K.A.Pericleous,S.N.Drake,1986][12]. The modelling is based on two suppositions: both phases share the same pressure field and the density of each phase is approximately constant. The governing equations used for mixture model are summarized below as: The

momentum equation Eqs(II.1), the continuity equation Eqs(II.2), Viscous and turbulent stresses Eqs(II.3), and transport equation for the dispersed phase Eqs(II.4) [S.T.Johansen,N. M.Anderson,1990][11][K.A.Pericleous,S.N.Drake,1986][12] :

$$\rho \mathbf{u}_t + \rho(\mathbf{u}\,.\,\nabla)\mathbf{u} = -\nabla \mathbf{p} - \nabla.\boldsymbol{\tau}_{Gm} - \nabla.\left[\rho \mathbf{c}_d(1-\mathbf{c}_d)\left(\mathbf{u}_{slip} - \frac{\mathbf{D}_{md}\ \nabla \emptyset_d}{(1-\mathbf{c}_d)\ \emptyset_d}\right)\left(\mathbf{u}_{slip} - \frac{\mathbf{D}_{md}\ \nabla \emptyset_d}{(1-\mathbf{c}_d)\ \emptyset_d}\right)^T\right] + \rho \mathbf{g} \quad \text{(II.1)}$$

$$\boldsymbol{\rho} + \nabla.(\boldsymbol{\rho}\mathbf{u}) = \mathbf{0} \quad \text{(II.2)}$$

$$\boldsymbol{\tau}_{Gm} = (\boldsymbol{\mu} + \boldsymbol{\mu}_T)\left[\left(\nabla \mathbf{u} + (\nabla \mathbf{u})^T - \frac{2}{3}(\nabla\,.\,\mathbf{u})\mathbf{I}\right)\right] \quad \text{(II.3)}$$

$$\frac{\partial}{\partial t}(\emptyset_d\,\rho_d) + \nabla.(\emptyset_d\,\rho_d\,\mathbf{u}_d) = -\mathbf{m}_{dc} \quad \text{(II.4)}$$

Where the density of mixture flow (ρ) is as:

$$\boldsymbol{\rho} = \emptyset_c\,\rho_c + \emptyset_d\,\rho_d \quad \text{And} \quad \emptyset_c = \mathbf{1} - \emptyset_d \quad \text{(II.5)}$$

The velocity (u) used in (1) is the mass-averaged mixture velocity, it defined as:

$$\mathbf{u} = \frac{\emptyset_c\,\rho_c\,\mathbf{u}_c + \emptyset_d\,\rho_d\,\mathbf{u}_d}{\rho} \quad \text{(II.6)}$$

The relation between the velocities $\mathbf{u_d}$ and $\mathbf{u_c}$ is defined by Eqs(II.7):

$$\mathbf{u_d} - \mathbf{u_c} = \mathbf{u_{slip}} - \frac{\mathbf{D_{md}}}{\emptyset_d(1-\mathbf{c_d})}\nabla \emptyset_d \quad \text{(II.7)}$$

u_{slip}: represents the relative velocities between the two phases. The relationship is as:

$$\frac{3\,C_d}{4\,d_d}\rho_c\,|\mathbf{u_{slip}}|\,\mathbf{u_{slip}} = -\frac{(\rho-\rho_d)}{\rho}(-\mathbf{u_t} - (\mathbf{u}.\nabla)\mathbf{u} + \mathbf{g}) \quad \text{(II.8)}$$

C_d is the coefficient of particle drag, it explained as the balance between the buoyancy force acting on the particles and the viscous drag, for the Schiller-Naumann drag model, $C_d = 0.44$.

In the mixture model the densities ρc and ρd of the two phases are supposed to be constant, consequently the following alternative equation form of continuity for the mixture flow becomes:

$$(\rho_c - \rho_d)\left\{\nabla\,.\,[\emptyset_d(1-\mathbf{c_d})\mathbf{u_{slip}} - \mathbf{D_{md}}\nabla \emptyset_d\,] + \frac{\mathbf{m_{dc}}}{\rho_d}\right\} + \rho_c\,(\nabla\,.\,\mathbf{u}) = \mathbf{0} \quad \text{(II.9)}$$

Equation (II.9) is derived from Equation (II.4) and Equation (II.2). Dmd(m2/s) is a turbulent dispersion coefficient that accounts for the additional diffusion required for turbulent vortices. It is defined by:

$$\mathbf{D_{md}} = \frac{\mu_T}{\rho\,\sigma_T} \quad \text{(II.10)}$$

$\boldsymbol{\sigma_T}$ (dimensionless) is the Schmidt number of turbulent particles. The particle Schmidt number has usually been suggested as a value in the range of 0.2 to 0.5. In physical applications,[A.N. Colli, J.M. Bisang,2018][13]. When there is no turbulence, Dmd is assumed to be zero. If the particle concentration is not high, the k-ε model can be applied to model the turbulence of multiphase flows. Corrections due to the dispersed phase to the normal single-fluid model have been develop [S.E.Elghobashi, T.W. AbouArab,1983] [A.Mostafa,.C.Mongia,1988][14] [A.Adeniji-Fashola,P.Chen,1990][15][The turbulent kinetic energy and the turbulent dissipation equations have to be solved as follows [S.T.Johansen,N.M. Anderson,1990][C.P.Chen,P.E.Wood,1985]:

$$\boldsymbol{\rho \frac{\partial k}{\partial t}} + \rho \mathbf{u} \,.\, \boldsymbol{\nabla k} = \boldsymbol{\nabla} \,.\, \left[\left(\boldsymbol{\mu} + \boldsymbol{\frac{\mu_T}{\sigma_k}}\right) \boldsymbol{\nabla k}\right] + \mathbf{P_k} - \boldsymbol{\rho \epsilon} \qquad \text{(II.11)}$$

$$\boldsymbol{\rho \frac{\partial \epsilon}{\partial t}} + \rho \mathbf{u} \,.\, \boldsymbol{\nabla \epsilon} = \boldsymbol{\nabla} \,.\, \left[\left(\boldsymbol{\mu} + \boldsymbol{\frac{\mu_T}{\sigma_\epsilon}}\right) \boldsymbol{\nabla \epsilon}\right] + \mathbf{c_{\epsilon 1}} \, \frac{\epsilon}{k} \, \mathbf{P_k} -$$

$$\mathbf{c_{\epsilon 2}} \, \boldsymbol{\rho} \, \frac{\epsilon^2}{k} \qquad \text{(II.12)}$$

Where Cμ=0.09, Cε1=1.44, Cε2=1.92, σk=1.0, and σε=1.3. P_k and μ_T are the production term and the mixture viscosity respectively, they are given as :

$$\boldsymbol{\mu_T} = \boldsymbol{\rho} \, \mathbf{c_\mu} \, \frac{k^2}{\epsilon} \qquad \text{(II.13)}$$

$$\mathbf{P_k} = \boldsymbol{\mu_T} \, [\boldsymbol{\nabla u} : (\boldsymbol{\nabla u} + (\boldsymbol{\nabla u})^{\mathbf{T}})] \qquad \text{(II.14)}$$

The so-called drift velocity is given as a diffusion term in Eq. (II.4) included:

$$\boldsymbol{\frac{\partial}{\partial t}} (\boldsymbol{\emptyset_d}) + \boldsymbol{\nabla} . (\boldsymbol{\emptyset_d} \, \boldsymbol{\beta}) = \boldsymbol{\nabla} . (\mathbf{D_{md}} \, \boldsymbol{\nabla \emptyset_d}) - \boldsymbol{\frac{m_{dc}}{\rho_d}} \qquad \text{(II.15)}$$

$$\boldsymbol{\beta_d} = \mathbf{u} + \mathbf{u_{slip}} \, (\mathbf{1} - \mathbf{c_d}) \qquad \text{(II.16)}$$

Correspondingly, the number density equation for turbulent flow corresponds to:

$$\boldsymbol{\frac{\partial n}{\partial t}} + \boldsymbol{\nabla} . (\mathbf{n} \, \boldsymbol{\beta_d}) = \boldsymbol{\nabla} . (\mathbf{D_{md}} \, \boldsymbol{\nabla n}) \qquad \text{(II.17)}$$

The viscous stress tensor includes an extra contribution, using the k-ε turbulence model, the Eq(II.3) is replaced by:

$$\boldsymbol{\tau_{Gm}} = (\boldsymbol{\mu} + \boldsymbol{\mu_T}) \left[\left(\boldsymbol{\nabla u} + (\boldsymbol{\nabla u})^{\mathbf{T}} - \frac{2}{3} (\boldsymbol{\nabla} \,.\, \mathbf{u}) \mathbf{I}\right)\right] - \frac{2}{3} \boldsymbol{\rho k I} \qquad \text{(II.18)}$$

Chapter III : Numerical Method and Simulation

The model is similar to previous experimental works [X.P.Liu,Z.B.Dong,2004][16], the simplified description

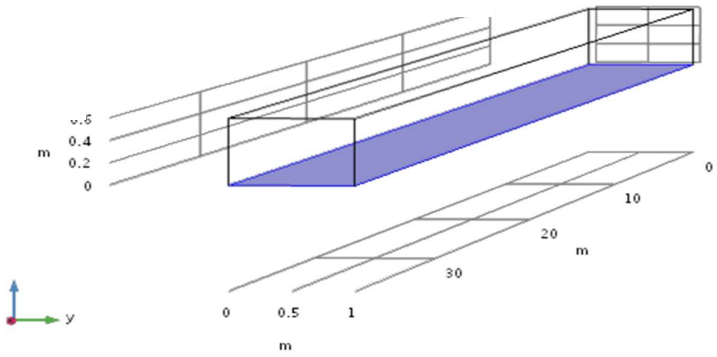

Figure III- 1 : The geometry of the computational domain

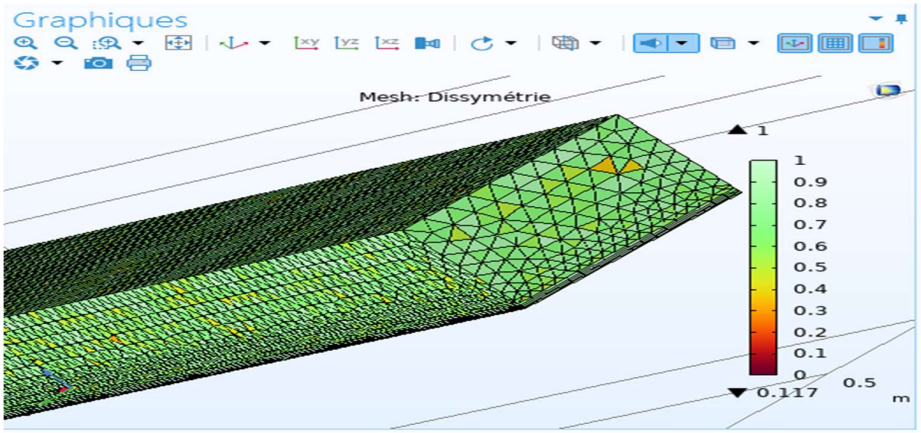

Figure III- 2 :meshing of the computational domain

The numerical simulation described here pertains to a 37.8-meter-long rectangular wind tunnel with cross-section areas of 1m and 0.6m. The air velocity u (m/s) at the inlet of the tunnel ranges from 10 to 12 m/s. Depending on the configuration of the erodible bed being examined, the tunnel floor is covered with sand of uniform height. Sand with mean diameters of 0.15 mm, density of ρ=2650 kg/m3. Since the Mach number is less than 0.05, the air, considered as the continuous phase, is treated as an incompressible gas. Turbulence intensity and turbulence length scale values are specified as 0.05 and 0.01m respectively, without considering the concentration of sand particles. At the outlet, the pressure is set to a reference value of Pref = 1 atm. Symmetrical boundary conditions are applied to both the air and sand phases. The complete mesh consists of 355228 domain elements, 28840 boundary elements, and 1564 edge elements.

III.1.1.Simulation

The numerical resolution was done by COMSOL Multiphysics is a finite element analyzer and simulation software package for various physics and engineering applications, especially coupled phenomena and Multiphysics.

III.1.2. COMSOL Multiphysics program:

We begin by entering the values we need in order to complete the study: length, depth, heigh.(We relied on these values based on previous experiences)

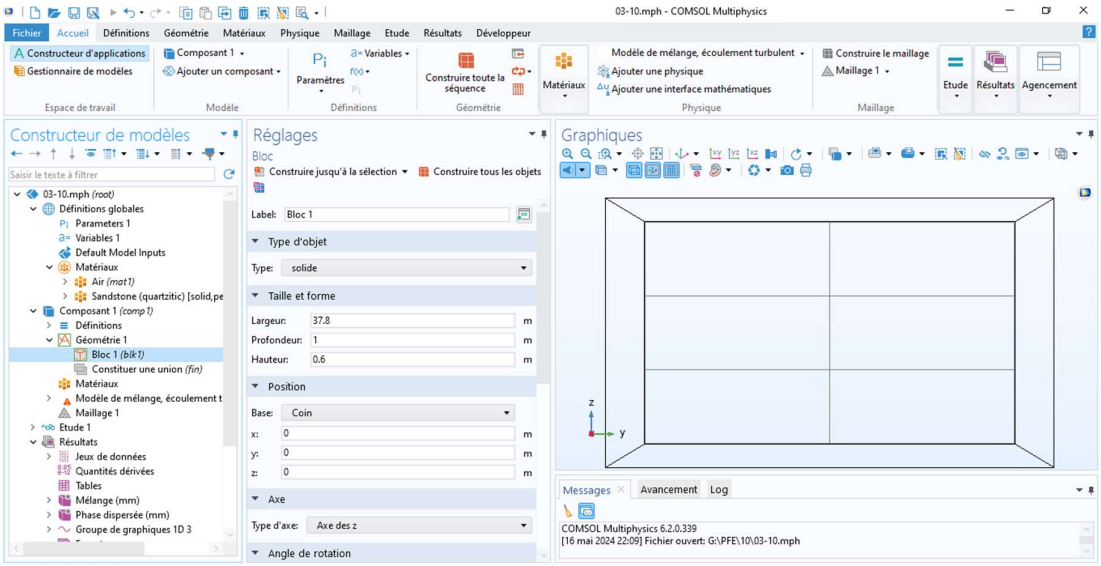

Figure III- 3:Entering the values in MATLAB

At this stage, we consider the Schmidt coefficient to be 0.3 and change its value after completing each simulation so that its value is, respectively, 0.6 0.9 and 1.2(Other variables are fixed)

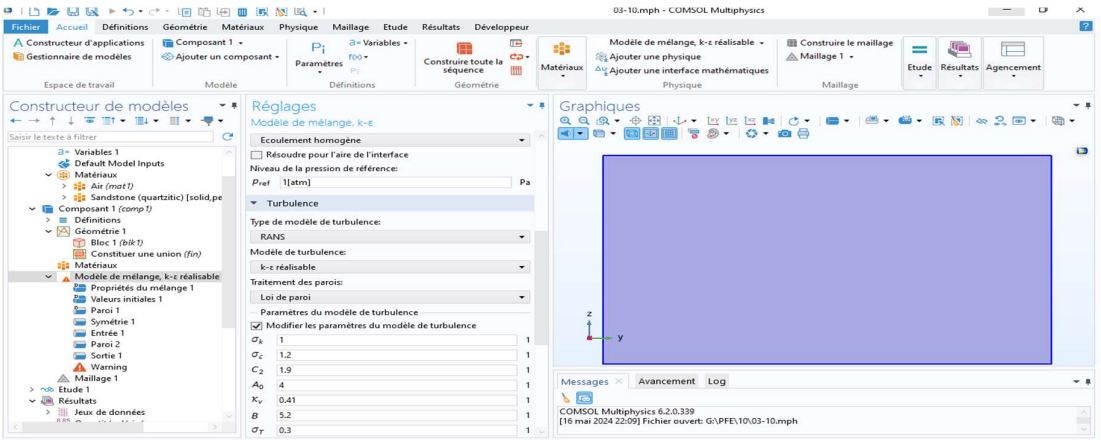

Figure III- 4: The Schmidt coefficient Sct=0.3

We name all the values we need at the end of the study

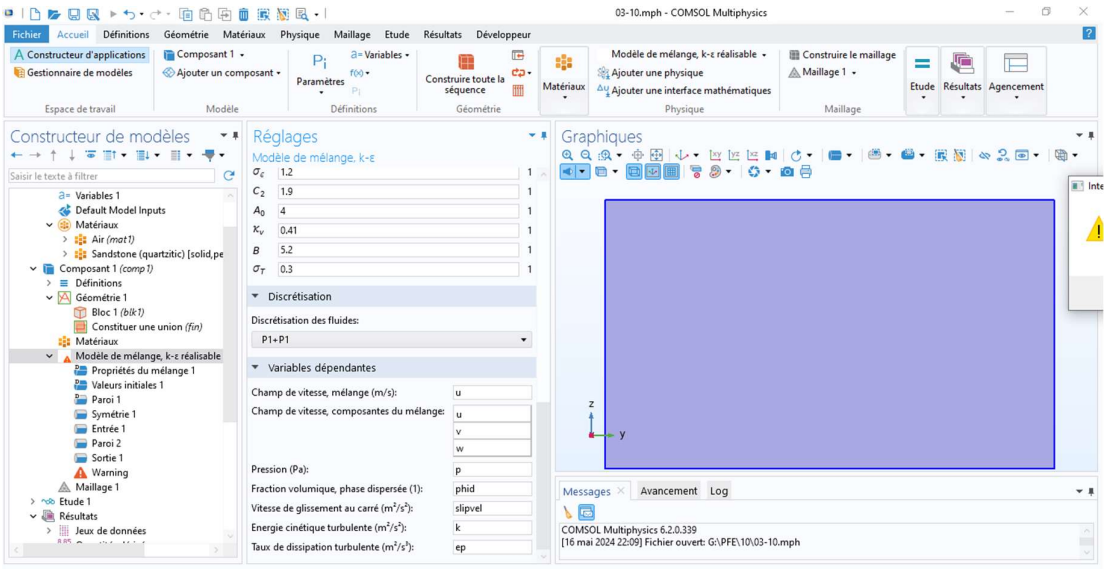

Figure III- 5: Name all values

We fix the speed value in the first study so that it is 10, and we change the Schmidt value between 0.3 0.6 0.9 1.2 and We keep the results obtained.Then we change the speed from 10 to 12 and each time we change the Schmidt coefficient as before

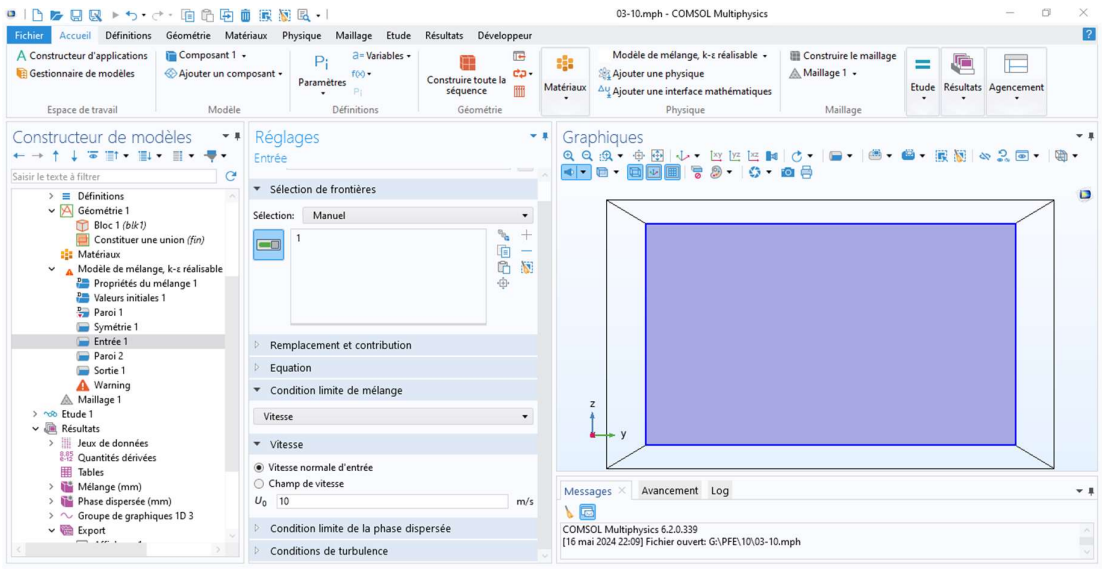

Figure III- 6: The speed of stady u=10m/s

Spatial distribution of the turbulent diffusion coefficient of particles

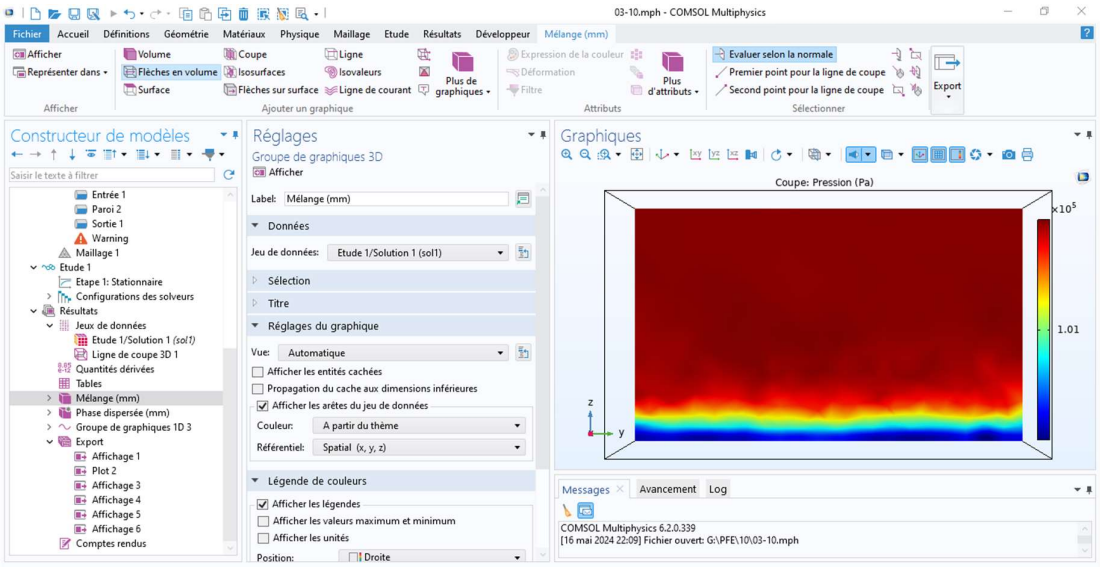

Figure III- 7:Spatial distribution of the turbulent diffusion coefficient of particles

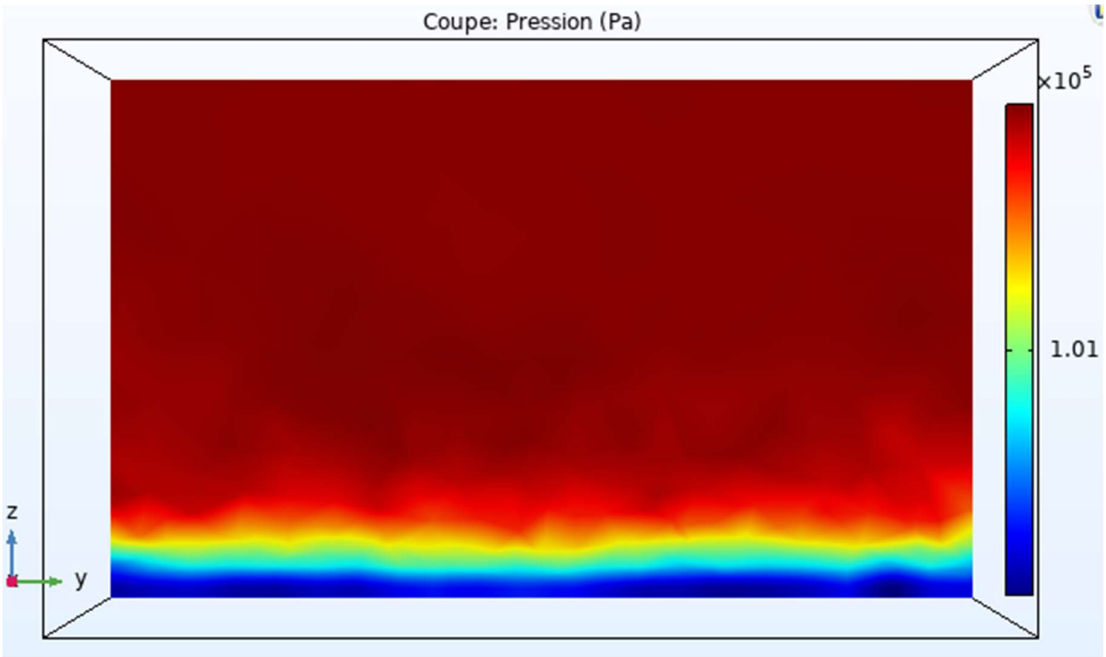

Figure III- 8:Image Spatial distribution of the turbulent diffusion coefficient of particles

A spatial sand concentration distribution

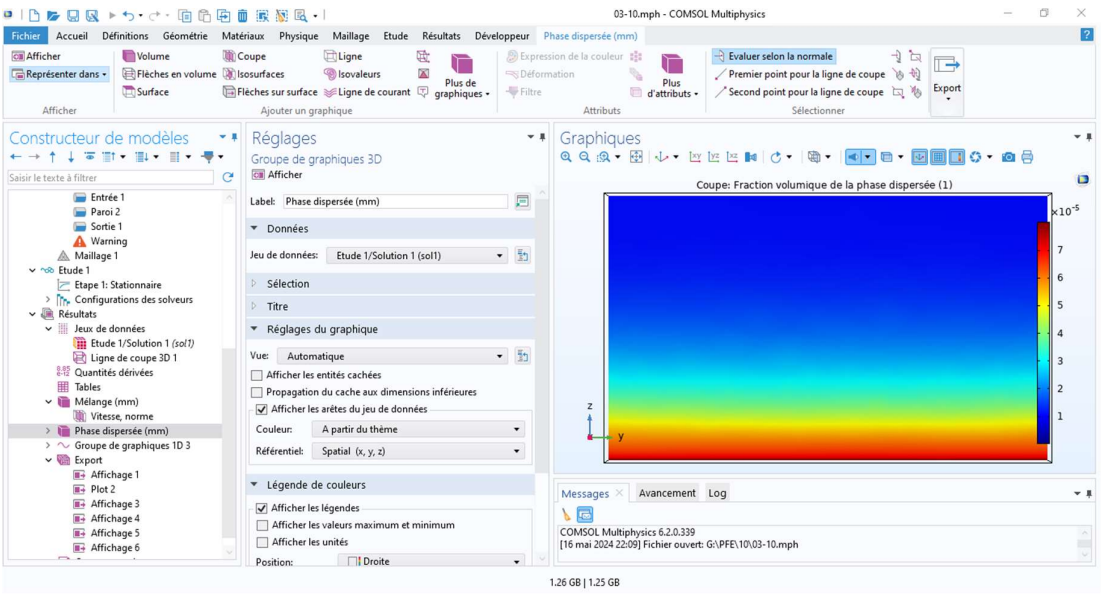

Figure III- 9:A spatial sand concentration distribution

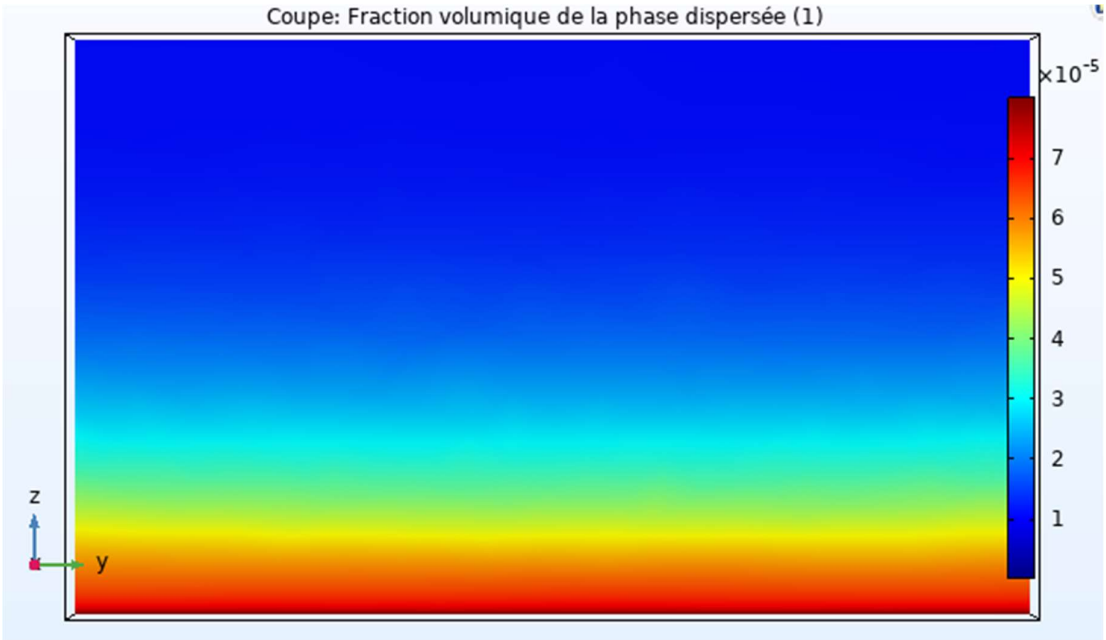

Figure III- 10:Image A spatial sand concentration distribution

After completing the simulation, we determine the curve to be studied:

When we choose the concentration in a box" Expression" the curve appears like this

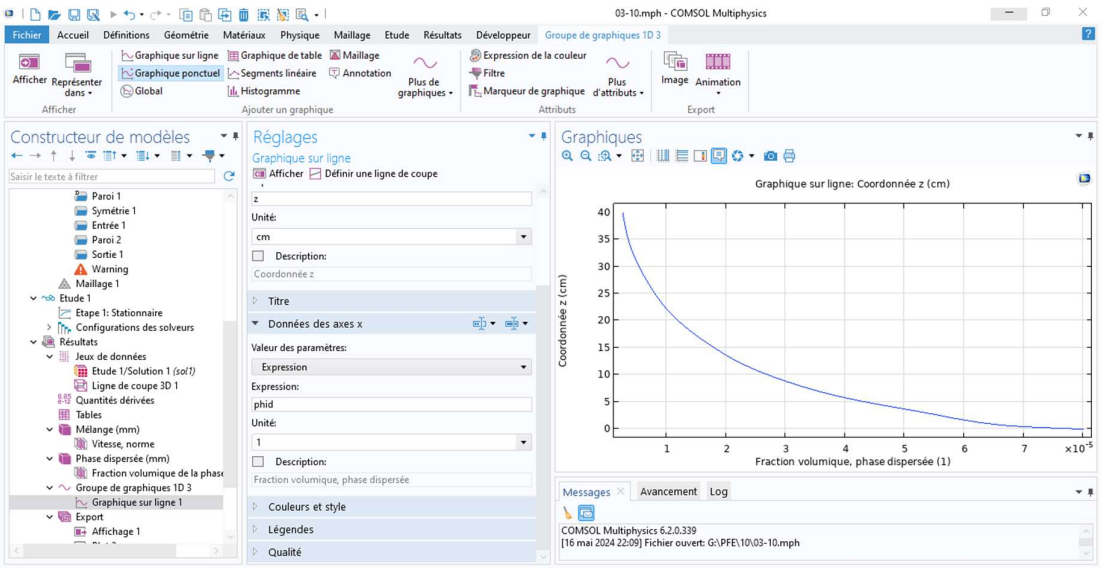

Figure III- 11:The curve of the concentration

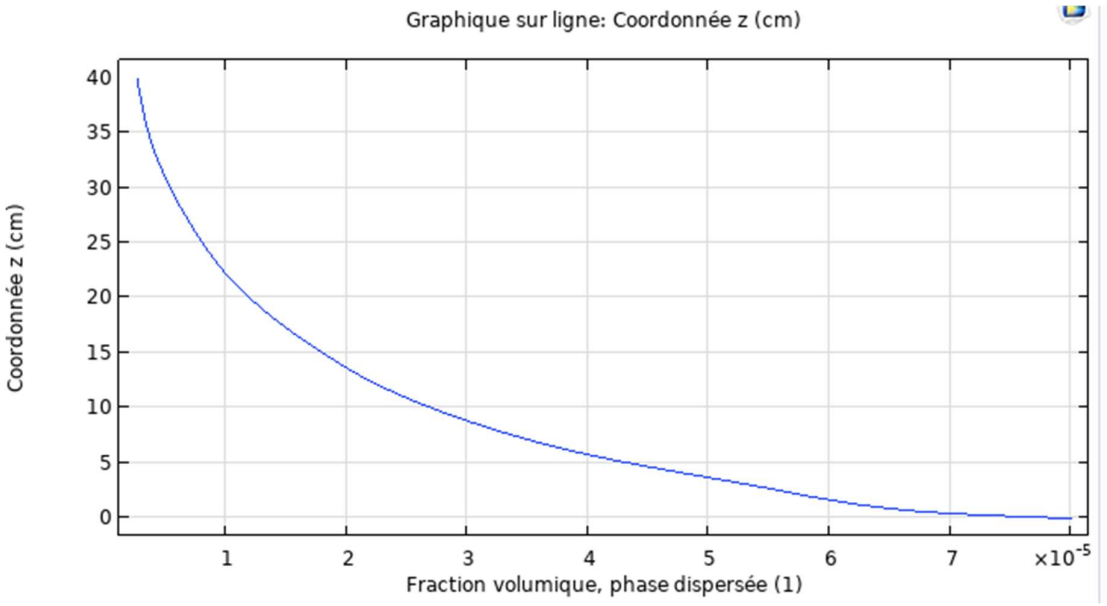

Figure III- 12 Photo The curve of concentration

When we choose diffusion in a box" Expression" the curve appears like this.

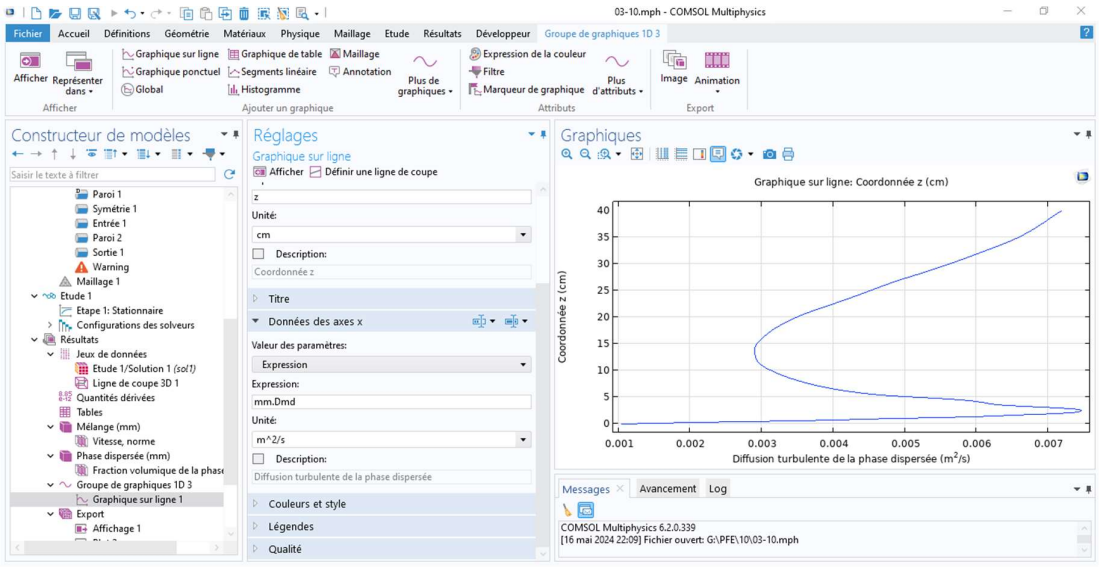

Figure III- 13:The curve of the diffusion

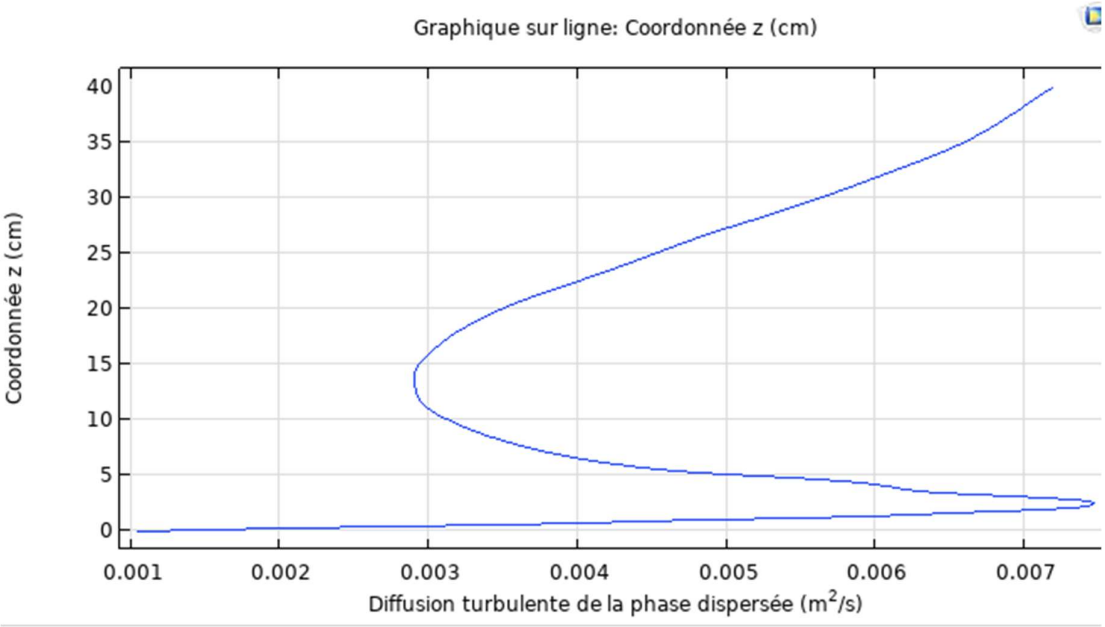

Figure III- 14:Photo The curve of the diffusion

COMSOL asks us for the type of file and the location of the file we want to obtain, which it converts into a matrix to transfer to the MATLAB program.

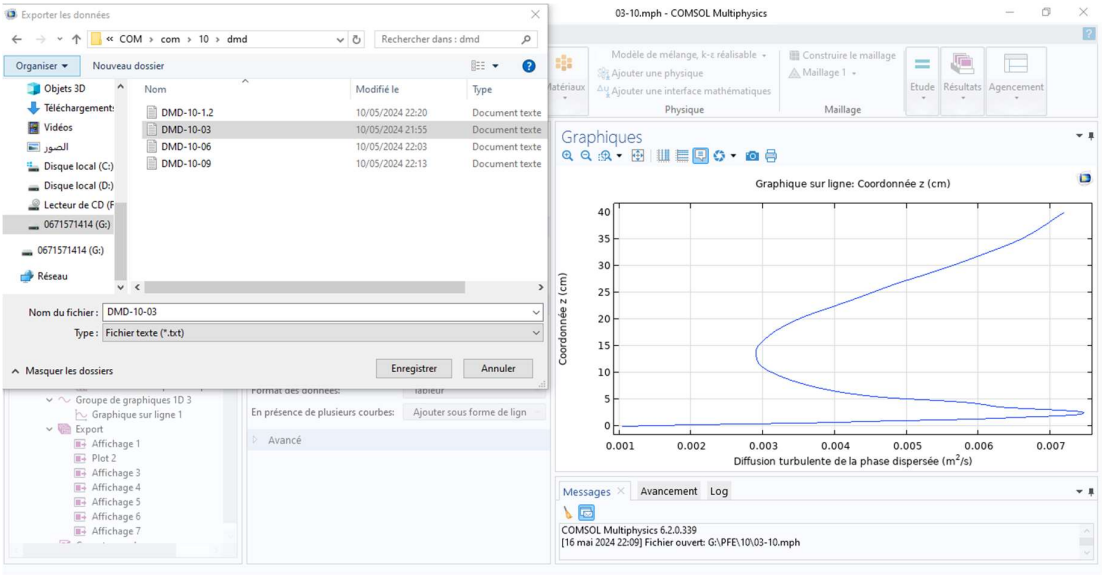

Figure III- 15:COMSOL asks us for the type of file and the location of the file we want to obtain

We save the file as a predicate

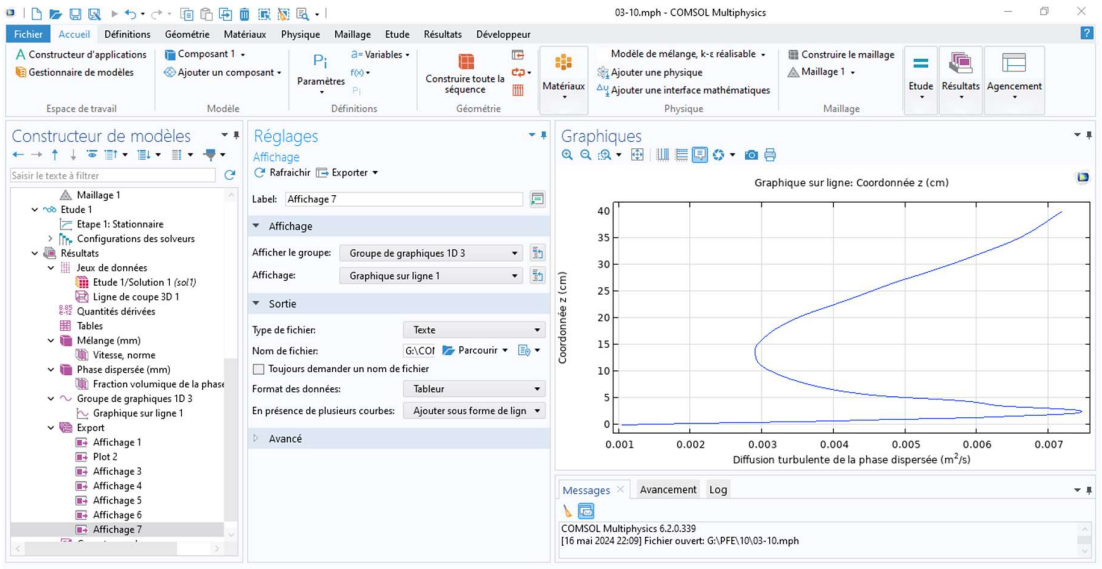

Figure III- 16:save the file as a predicate

III.1.3. MATLAB program:

After saving the file, we open the MATLAB application, and then we start creating an equation each time that includes the matrix obtained after each simulation

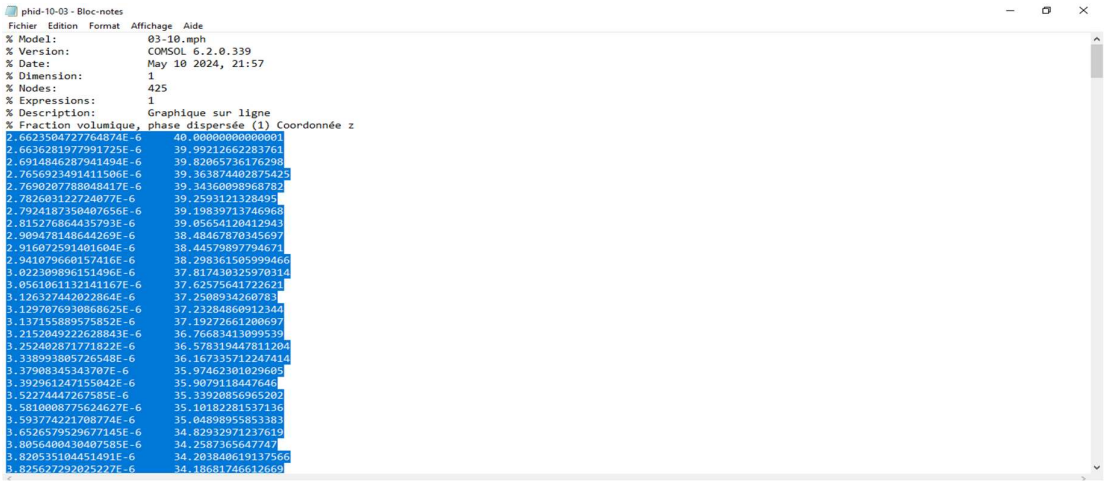

Figure III- 17:the matrix obtained after each simulation

First, we choose the results obtained when setting the speed to 10 and changing the Schmidt number , Secondly, we create another file and take the results obtained at speed 12 and change the Schmidt number .

Then we choose the appropriate equation to draw a simulation of the curve corresponding to the study each time

When studying the diffusion, we choose Gaussian the second degree to obtain the curve and the results obtained

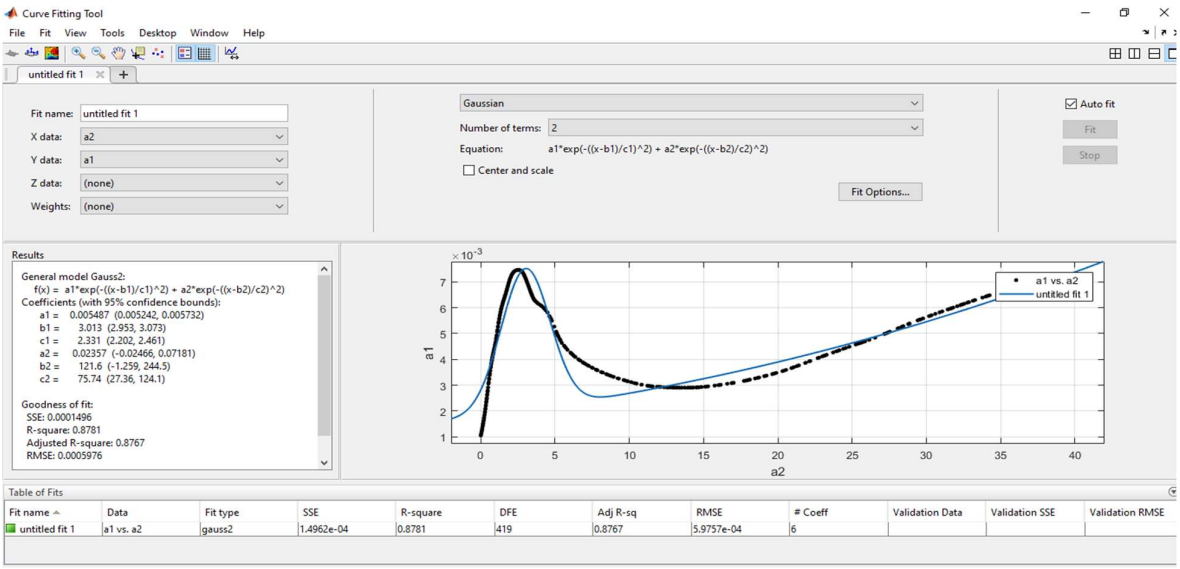

Figure III- 18:Gaussian the second degree to obtain the curve and the results obtained

When studying the concentration, we choose Exponential the first degree to obtain the curve and the results obtained

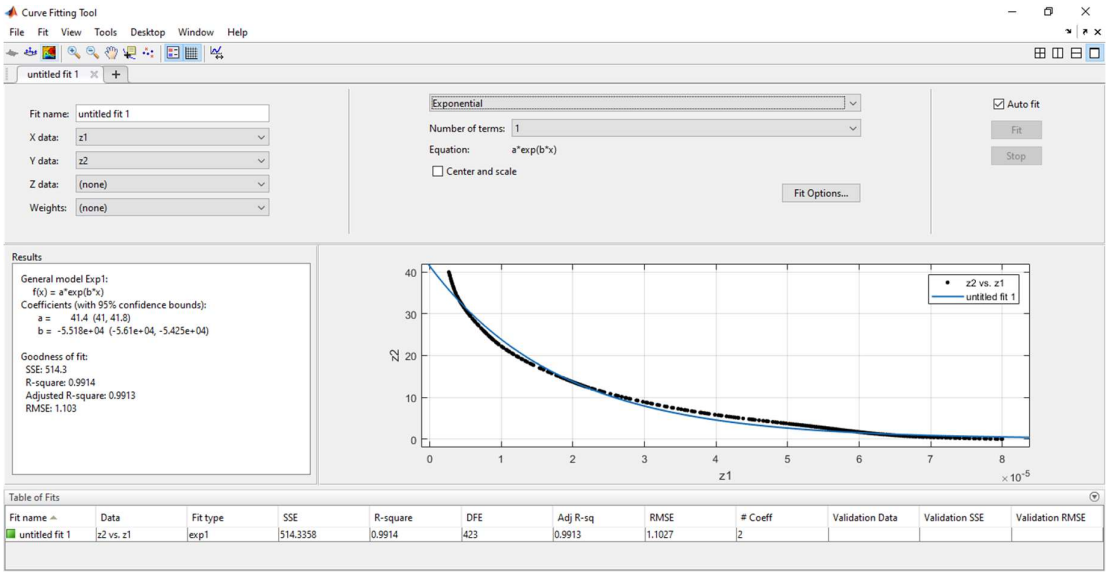

Figure III- 19:Exponential the first degree to obtain the curve and the results obtained

Each time, we copy the equation and the results obtained and place them in an incoming document that includes variable results as the Schmidt number changes.

We take, for example, the diffusion changes at Sct=0.3 Sct= 0.6 Sct=0. 9 Sct= 1.2 where the velocity u = 10 m/s

So, we get the following MATLAB program

```
a1 =      0.005515   ;
       b1 =   3.013   ;
       c1 =      2.332  ;
       a2 =    0.01976  ;
       b2 =        111   ;
       c2 =        71.45  ;
       x=linspace(0.005,20,800);
      f =  a1.*exp(-((x-b1)./c1).^2) + a2.*exp(-((x-b2)./c2).^2);
       plot(x,f)
       hold on
       a3 =      0.002791  ;
       b3 =       2.993  ;
       c3 =     2.378  ;
       a4 =    0.006901  ;
       b4 =       87.27  ;
       c4 =       59.73  ;
      f1 =  a3.*exp(-((x-b3)./c3).^2) + a4.*exp(-((x-b4)./c4).^2);
       plot(x,f1)
       hold on
        a5 =    0.008642;
       b5 =     65.17  ;
       c5 =     44.81  ;
       a6 =     0.003462  ;
       b6 =      3.095  ;
       c6 =       2.645  ;
      f2 =  a5.*exp(-((x-b5)./c5).^2) + a6.*exp(-((x-b6)./c6).^2);
       plot(x,f2)
       hold on
        a6 =   0.00301;
       b6 =     75.13   ;
       c6 =     49.58  ;
       a7 =      0.001216  ;
       b7 =      3.238  ;
       c7 =       2.789  ;
      f3 =  a6.*exp(-((x-b6)./c6).^2) + a7.*exp(-((x-b7)./c7).^2);
       plot(x,f3)
       hold on
```

We copy the obtained equations and place them in a MATLAB file

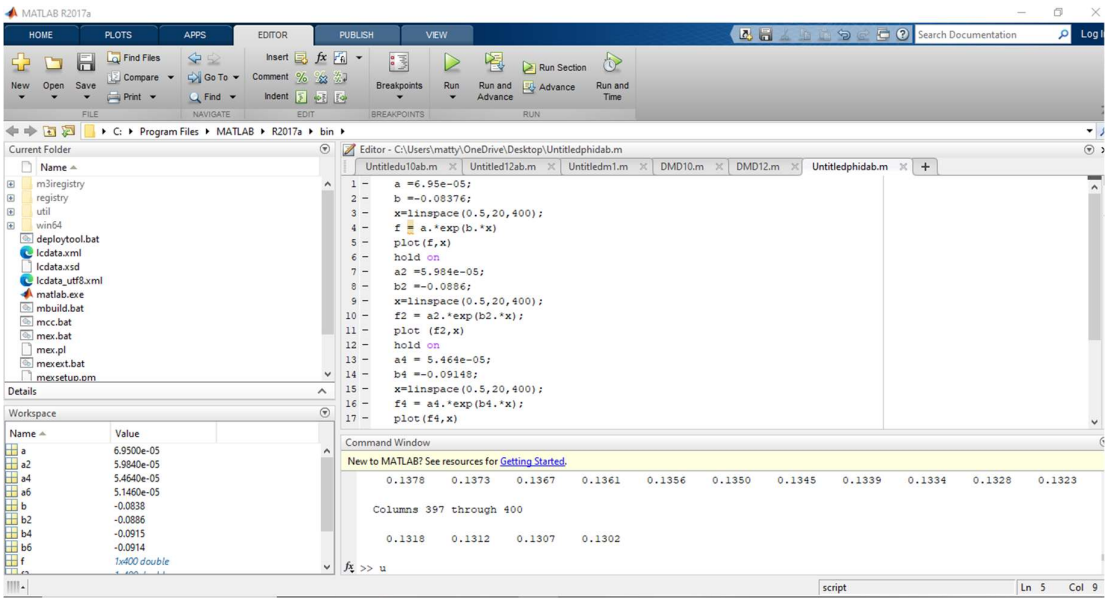

Figure III- 20:Equations final in a MATLAB

When all the steps are completed, we set the speed to 10, change the Schmidt number to (0.3 0.6 0.9 and 1.2) and draw the curves .Then we change the speed(u=12m/s), change the Schmidt number to (0.3 0.6 0.9 and 1.2), and draw the curves.

Finally, When we obtain the curves, we can analyze the results and study this phenomenon.

Chapter IV : Results and discussion

IV.1. Turbulent diffusion coefficient of Sand particules :

IV.1.1. Study the phenomenon

The illustrates an example of the spatial distribution of the diffusion of the turbulent particle in the Z–Y plane at u=10 m/s and dp = 0.15 mm. From this Figure, it can be seen that within the boundary layer (z<6cm) the diffusivity of sand particles increases and decrease rapidly with height. Outside the boundary layer, the diffusion coefficient increases slowly with increasing height

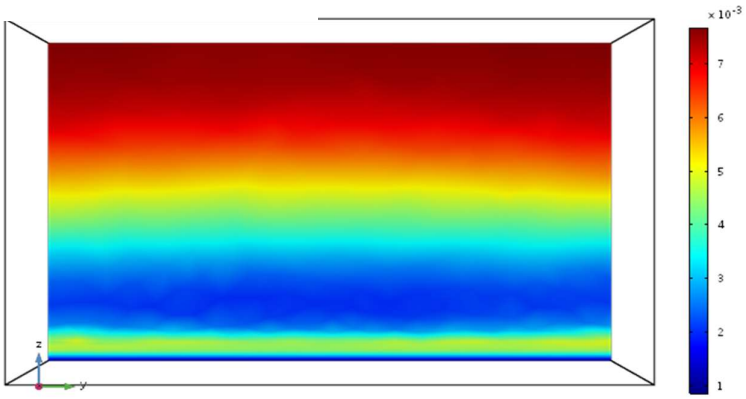

Figure IV- 1 : Spatial distribution of the turbulent diffusion coefficient of particles in the Z–Y plane at u=10 m/s and dp = 0.15 mm

Physically, σT represents the ratio between the viscous diffusion rate (linked to ν) and the mass diffusion rate or diffusion coefficient (Dmd). It can also describe the relationship between the rates of turbulent momentum transport and turbulent mass transport[C. M.Tchen,1947], from the CFD simulations and experimental data, σT ranges from 0.3 to1.2 . In our simulation,

we take the turbulent Schmidt number as 0.3 ,0.6 ,0.9 and 1.2.

The variation of diffusion coefficient with height can be written as a Gaussian distribution with the squared correlation coefficient R2=0.90, it can be written as:

$$D_{md} = a \,.\, e^{\left(-\left(\frac{z-b}{c}\right)^2 + a_1 e^{-\left(\frac{z-b_1}{c_1}\right)^2}\right)} \qquad \text{(IV.1)}$$

IV.1.2. Curves:

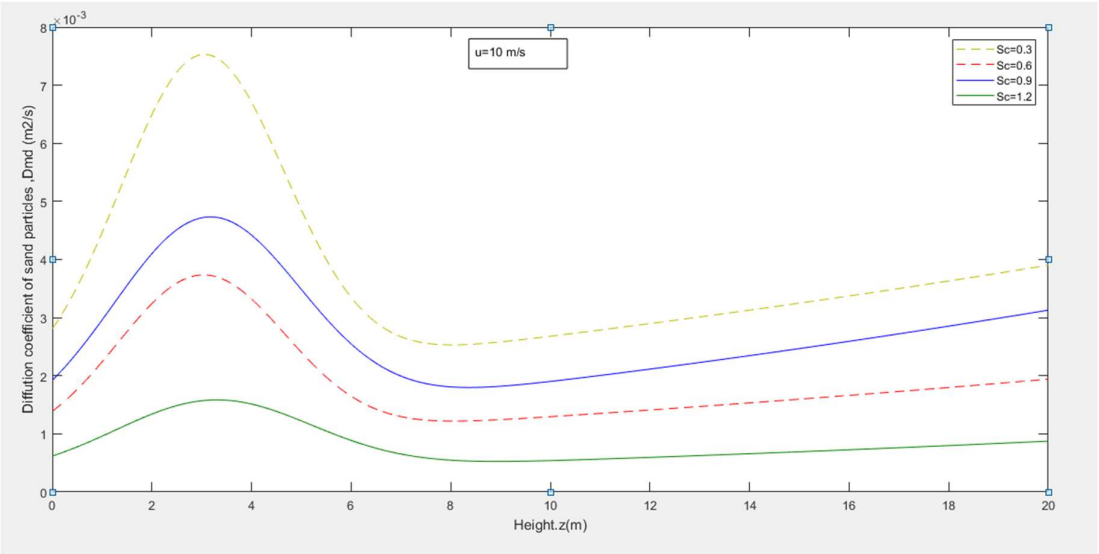

Figure IV- 2 : Vertical values of particles diffusion coefficient for different Sct: 0.3 0.6 0.9 1.2 (u=10m/s)

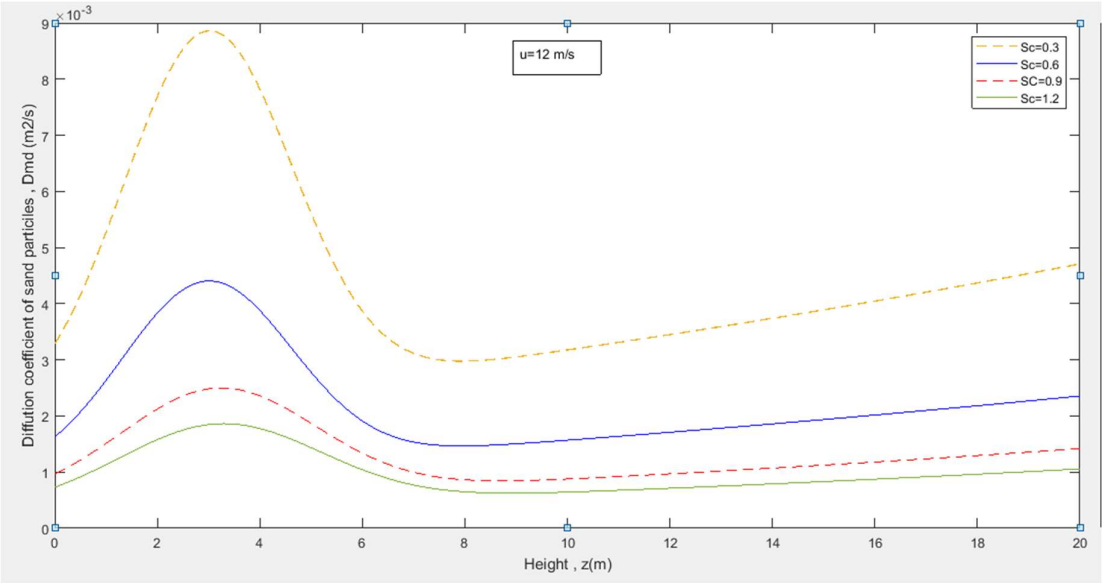

Figure IV- 3 : Vertical values of particles diffusion coefficient for different Sct: 0.3 0.6 0.9 1.2 (u=12m/s)

IV.1.3. Analysis of the results

The graph can be divided into two parts:

- The first, internal part can be described by Gaussian

-The second part is external which is expressed by a linear function.

The first part, It can also be observed that the maximum value for diffusion is that whenever Sct changes, the value of diffusion changes and its value reaches a peak. This means that Sct directly affects the diffusion values, despite the speed being fixed at 10 m/s.

Second part: Whenever St changes, the diffusion value changes in as a constant linear function, and we notice that the diffusion values converge between the two values corresponding to St = 0.6 and St = 0.9.When the speed is fixed at 10m/s.

While there is a convergence in the values of Sct = 0.3 and Sct = 0.6 when the speed is fixed at 12 m/s

IV.2. Variation of the concentration of particles in mixture flow

IV.2.1. Study the phenomenon

A representative view of the sand concentration distribution is shown in (Figure IV-4). It turns out that the concentration of the sand is not homogeneously distributed in the Z-Y plane, also it can be observed that more than half of the sand flux is concentrated at an elevation that occupies about 20% of the total thickness of the sand bed

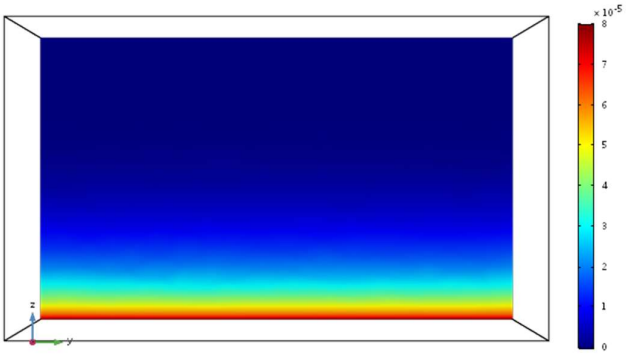

Figure IV- 5 : A spatial sand concentration distribution (Ø_d) on the Y-Z plane at u=10 m/s and dp = 0.15 mmA spatial sand concentration distribution (Ø_d) on the Y-Z plane at u=10 m/s and dp = 0.15 mm

Here again, to validate the reliability of our simulation results based on mixture theory, the published data of concentration

profile of sand particles at similar experimental conditions were used in this study [X.P. Liu, Z.B.Dong,2004]

It may indicate that the shape and type of particles of sand used in this simulation were spherical quartz, whereas the shape and type used in the experimental was natural sand, moreover the experimental conditions were not the same as the work of this study. Vertical profiles of particle densities for different velocities are shown in Fig.5. The height (z) is measured from the surface of the sand bed. For different values of Sct , the particle density decays rapidly with height. The regression of particle volume fraction shows that the concentration of all grain sizes of sand particles and wind velocities decreases exponentially with height [X.P. Liu, Z.B. Dong,2004] [Z.Y, Liu, J.J. Zhu,1998] [17] as:

$\emptyset_{\mathbf{d}}$ = a. $\boldsymbol{e^{-bz}}$ (IV.2)

$\emptyset_{\mathbf{d}}$: Denote the particle density at height z. a and b are coefficients of fitted function regression. the Eqs(IV.2) fits well to the simulation results , with R2 = 0.97 to 0.99. The suspension effect is negligible while the diameters of grain sand used are greater than 0.1mm. The findings show that the sand concentration in the saltation layer can be characterized by the natural of the exponential function.

The findings show that the sand concentration in the saltation layer can be characterized by the natural of the exponential function. Denote that the particle density close to the sand bed is in the order of 10-5 .

The coefficient (a) in Eq (IV.2) represents the density at the sand bed, it decreases with grain diameter size but increases with wind velocity . The coefficient (b) correlates with the slope of the straight line. The variability of coefficient b shows that more sand is moved to higher height level as both wind velocity and sand grain diameter size increase.

IV.2.3. Curves:

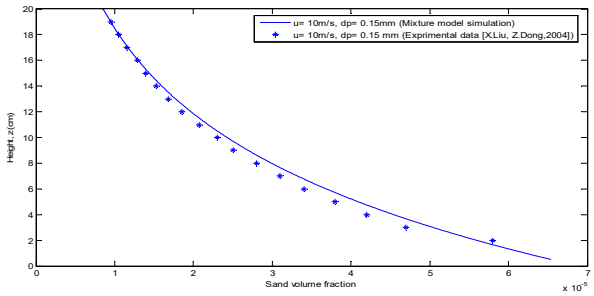

Figure IV- 6 :Comparison of concentration profile with experimental data of [X.P. Liu, Z.B. Dong,2004]

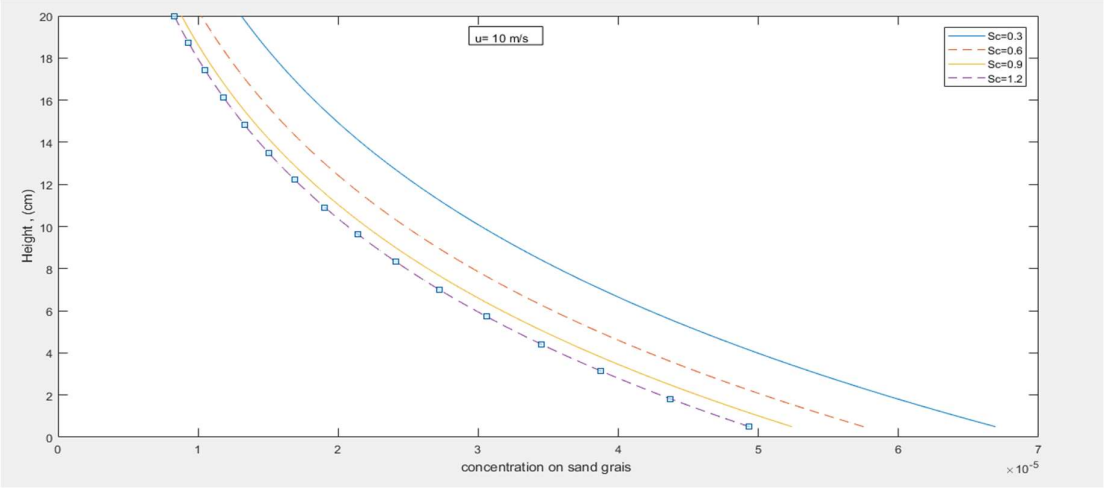

Figure IV- 7 : Comparison of concentration profile with experimental data of Liu and Dong (2004) (u=10m/s)

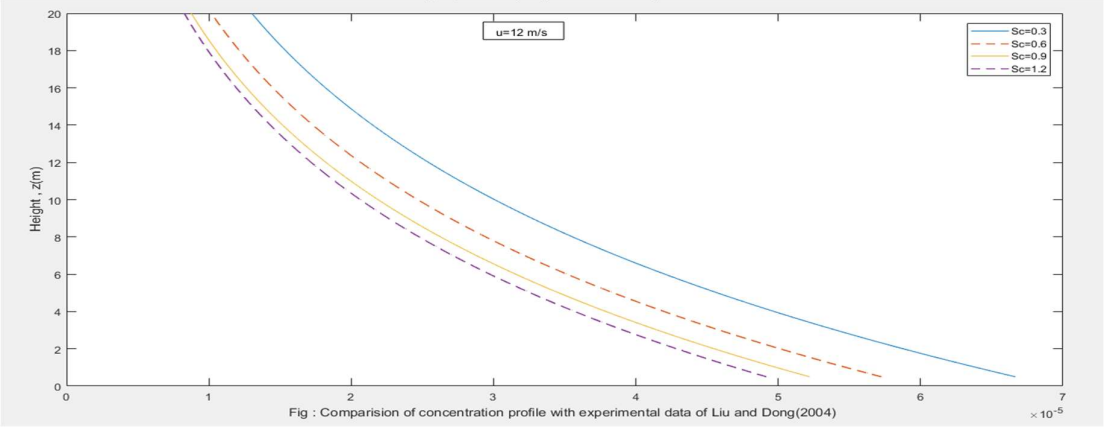

Figure IV- 8 : Comparison of concentration profile with experimental data of Liu and Dong (2004) u=12m/s

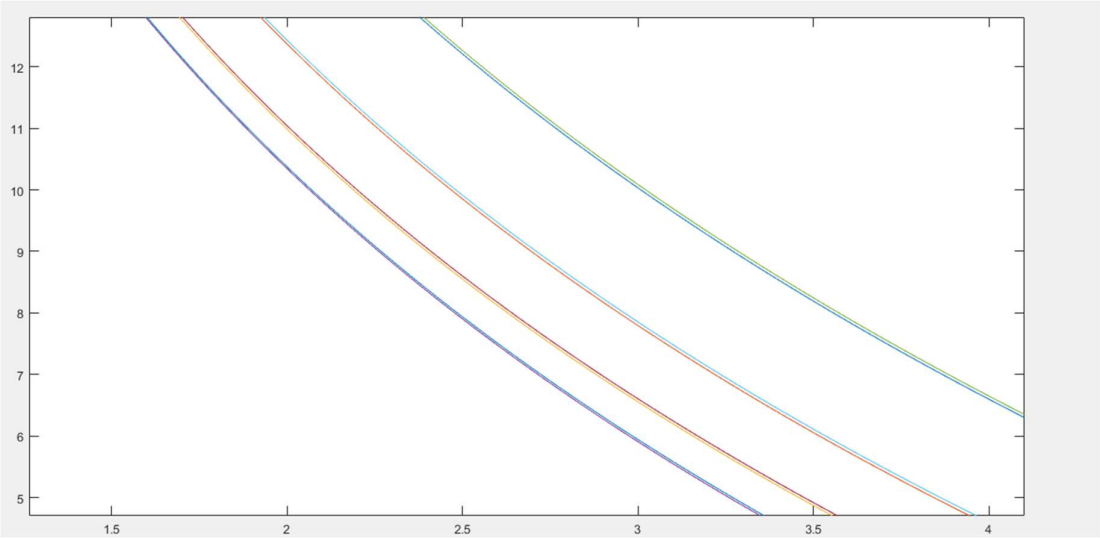

Figure IV- 9 :concentration profile (u=10m/s and u=12m/s)

IV.2.4. Analysis of the results :

We notice from the two curves that they are almost identical despite the change in speed (u= 10 m/s , u= 12m/s) and from this we conclude that the Schmidt number does not directly affect the concentration.

Conclusion

In this work, numerical simulation of Study of the nature of the particle distribution coefficient function in the boundary layer of the sand cloud. COMSOL Multiphysics was used for numerical analysis governing equations. The results obtained are in good agreement with experimental and numerical works.

Based on the results obtained from the different diffusion values diffusion we conclude that Schmidt number Sct=0.6 is the most approximate value for the studied phenomenon.

Concentration does not significantly affect the studied phenomenon when changing the Schmidt number (Sc=0.3, 0.6, 0.9, 1.2) or velocity (u=10m/d ,12 m/s)

The diffusion coefficient of sand particles was related to the form of the dispersed phase (sand grain sizes) and the kinetic energy of surrounding gas. The higher wind velocities allowed the sand particles to disperse on the air more than compared with the lower wind velocities.

Finally, we are the experts who consider this work useful for scientific research and well approaching the idea of studying this phenomenon.

References

[1] Hadjaissa Aissa. CONCENTRATION AND TURBULENT DIFFUSIVITY OF SAND PARTICLES IN THE ATMOSPHERE BASED ON MIXTURE MODEL THEORY A. International Journal of Fluid Mechanics Research, 2023

[2] Craig R. Sloss, Patrick Hesp & Michael Shepherd. Coastal Dunes: Aeolian Transport . 2012 Nature Education

[3] Koeltzsch, K. The height dependence of the turbulent Schmidt number within the boundary layer. Atmos. Environ. 2000, 34, 1147–1151

[4] Tominaga, Y.; Stathopoulos, T. Turbulent Schmidt numbers for CFD analysis with various types of flowfield. Atmos. Environ. 2007, 41, 8091–8099.

[5] Riddle, A.; Carruthers, D.; Sharpe, A.; McHugh, C.; Stocker, J. Comparisons between FLUENT and ADMS for atmospheric dispersion modelling. Atmos. Environ. 2004, 38, 1029–1038.

[6] Di Sabatino, S.; Buccolieri, S. MUST experiment simulations using CFD and integral models. In Proceedings of the 11th International Conference on Harmonisation within Atmospheric Dispersion Modelling for Regulatory Purpose, Cambridge, UK, 2–5 July 2007. 4-27

[7] Galeazzo Cunha, F.C.; Donnert, G.; Cárdenas, C.; Sedlmaier, J.; Habisreuther, P.; Zarzalis, N.; Beck, C.; Krebs, W. Computational modeling of turbulent mixing in a jet in crossflow. Int. J. Heat Fluid Flow 2013, 41, 55–65.

[8] Goldberg, U.; Palaniswamy, S.; Batten, P.; Gupta, V. Variable turbulent Schmidt and Prandtl number modeling. Eng. Appl. Comput. Fluid Mech. 2010, 4, 511–520.

[9] Shi, Z.; Chen, J.; Chen, Q. On the turbulence models and turbulent Schmidt number in simulating stratified flows. J. Build. Perform. Simul. 2016, 9, 134–178.

[10] D.Gidaspow,1994Ishii, M., Thermo-fluid Dynamic Theory of Two-phase Flow, Springer New York, NY, 2010. Jenkins, J. and Cantat, I. and Valance, A., Continuum model for steady, fully developed saltation above a horizontal particle bed, Phys. Rev. E82 020301R, 2009. https://doi.org/10.1103/PhysRevE.82.020301 29-4

[11] Johansen, S. and Anderson, N. and De Silva, S., A two-phase model for particle local equilibrium applied to air classification of powers, Power Technology, Vol. 63, pp. 121 – 132, 1990. 5-29-/1-30/6-31

[12] Pericleous, K. and Drake, S., An Algebraic Slip Model of PHOENICS for Multi-phase Applications, Numerical Simulation of Fluid Flow and Heat/Mass Transfer Processes Lecture Notes in Engineering vol 18. Springer, Berlin, Heidelberg, 1986. https://doi.org/10.1007/9783-642-82781-5-29_6-29 2 -30

[13] Colli, A. and Bisang, J., A CFD Study with Analytical and Experimental Validation of Laminar and Turbulent Mass-Transfer in Electrochemical Reactors, Journal of The Electrochemical Society, Volume 165, Number 2, 2018 31.1

[14] Mostafa, A. and Mongia, C., On the interaction of particles and turbulent fluid flow, Int. J. Heat Mass Transfer, Vol. 31, No. 10, pp. 2063 – 2075, 1988. 3-31

[15] Adeniji, A. and Chen, C., Modeling of confined turbulent fluid-particle flows using Eulerian and Lagrangian schemes, Int. J. Heat Mass Transfer, Vol. 33, No. 4, pp. 691 – 701, 1990. Ahmadi, G. and Ma, D., A thermodynamical formulation for dispersed multiphase turbulent flows Basic theory, Int. J. Multiphase Flow, Vol. 16, No. 2, pp. 323 – 340, 1990. 31.4

[16] Liu, X. and Dong, Z., Experimental investigation of the concentration profile of a blowing sand cloud, J.Geomorphology 60 . 371–381,2004. 32

[17] Liu, Z. and Zhu, J. and Kuang, Z., Saltation in windblown sand, Sci. China Ser. A-Math. 41, 629–637, 1998 https://doi.org/10.1007/BF02876233 47

[18] AAAA

[19] https://en.wikipedia.org/wiki/Aeolian_processes

[20] Leo C. van Rijn Aeolian sand transport processes, Part 1: model formulation and calibration www.leovanrijn-sediment.com

[21] Carlo Gualtieri 1,*, Athanasios Angeloudis 2, Fabian Bombardelli 3, Sanjeev Jha 4 and Thorsten Stoesser On the Values for the Turbulent Schmidt Number in Environmental Flows

[22] https://en.wikipedia.org/wiki/Schmidt_number